
Genetic diversity of the harmful family Kareniaceae (Gymnodiniales, Dinophyceae) in France, with the description of *Karlodinium gentienii* sp. nov.: A new potentially toxic dinoflagellate

Nézan Elisabeth^{1,*}, Siano Raffaele², Boulben Sylviane¹, Six Christophe^{3,4}, Bilién Gwenael¹, Cheze Karine⁵, Duval Audrey¹, Le Panse Sophie⁶, Quéré Julien², Chomérat Nicolas¹

¹ IFREMER, Station de Biologie Marine, Place de la Croix, BP 40537, F-29185 Concarneau Cedex, France

² IFREMER, Centre de Bretagne, DYNECO/Pelagos, BP 70, F-29280 Plouzané, France

³ Sorbonne Universities, Pierre et Marie Curie University (Paris 06), UMR 7144, Marine Phototrophic Prokaryotes Group, Station Biologique de Roscoff, 29688 Roscoff Cedex, France

⁴ Centre National pour la Recherche Scientifique, UMR 7144, Marine Phototrophic Prokaryotes Group, Station Biologique de Roscoff, Place Georges Teissier, CS90074, 29688 Roscoff Cedex, France

⁵ Muséum National d'Histoire Naturelle, Station de Biologie Marine, BP 225, F-29182 Concarneau Cedex, France

⁶ Centre National pour la Recherche Scientifique, Fr 2424, Plate-forme Merimagerie, Station Biologique de Roscoff, Place Georges Teissier, CS90074, 29688 Roscoff Cedex, France

* Corresponding author : Elisabeth Nézan, tel.: +33 298104280 ; fax: +33 298104281 ; email address : elisabeth.nezan@ifremer.fr

Abstract :

The family Kareniaceae is mostly known in France for recurrent blooms of *Karenia mikimotoi* in the Atlantic, English Channel, and Mediterranean Sea and for the unusual green discoloration in the saltwater lagoon of Diana (Corsica) caused by *Karlodinium corsicum* in April 1994. In terms of diversity, this taxonomic group was long overlooked owing to the difficult identification of these small unarmored dinoflagellates. In this study, thanks to the molecular characterization performed on single cells from field samples and cultures, twelve taxonomic units were assigned to the known genera *Karenia*, *Karlodinium* and *Takayama*, whereas one could not be affiliated to any described genus. The molecular phylogeny inferred from the D1–D2 region of the LSU rDNA showed that five of them formed a sister taxon of a known species, and could not be identified at species-level, on the basis of molecular analysis only. Among these latter taxa, one *Karlodinium* which was successfully cultured was investigated by studying the external morphological features (using two procedures for cells fixation),

ultrastructure, pigment composition, and haemolytic activity. The results of our analyses corroborate the genetic results in favour of the erection of *Karlodinium gentienii* sp. nov., which possesses an internal complex system of trichocysts connected to external micro-processes particularly abundant in the epicone, and a peculiar pigment composition. In addition, preliminary assays showed a haemolytic activity.

Highlights

► The diversity of the Kareniaceae in France was genetically studied. ► A taxon from the Atlantic clustered with a Dinophyceae from Antarctica in a new clade. ► *Karenia brevisulcata* and *K. umbella* were unexpectedly detected. ► The new potentially toxic dinoflagellate *Karlodinium gentienii* was described. ► *K. gentienii* showed a complex trichocyst system and a peculiar pigment composition.

Abbreviations

- LBS, ML bootstrap support;
- BPP, Bayesian posterior probabilities

Keywords : Genetic diversity, Haemolytic, Kareniaceae, Pigments, Single cell, Taxonomy

1. Introduction

The family Kareniaceae of the order Gymnodiniales has been erected to encompass unarmored dinoflagellates whose chloroplasts contain fucoxanthin and/or fucoxanthin-derivatives, and which possess a straight or sigmoid apical groove (Bergholtz et al., 2005). It includes the genera *Karenia* G. Hansen et Moestrup, *Karlodinium* J. Larsen and *Takayama* de Salas, Bolch, Botes et Hallegraeff, to which several unarmored dinoflagellates previously classified under the large genera *Gymnodinium* Stein and *Gyrodinium* Kofoid et Swezy are affiliated (Daugbjerg et al., 2000; de Salas et al., 2003). Mortality and ichthyotoxicity phenomena have been described worldwide for a long time, associated to recurrent blooms of *Karenia brevis* (Davis) G. Hansen et Moestrup in North America (Landsberg and Steidinger, 1998), *Karenia mikimotoi* (Miyake et Kominami ex Oda) G. Hansen et Moestrup in Japan, Europe, Australia and New Zealand (Takayama and Adachi, 1984; Dahl and Tangen, 1993; Hallegraeff, 2002), *K. selliformis* Haywood, Steidinger et MacKenzie in Tunisia and Chile (Clément et al., 2001; Medhioub et al., 2009), *Karlodinium veneficum* (Ballantine) J. Larsen in North America, Australia and Europe (Deeds et al., 2002; Kempton et al., 2002; Garcés et al., 2006; Hallegraeff et al., 2010; Place et al., 2012). Finally, an extremely toxic bloom of *Karenia brevisulcata* devastated all marine life in 1998 in New Zealand (Chang, 1999).

In France, the Kareniaceae family is mostly known for recurrent blooms of *K. mikimotoi* (previously recorded as *Gyrodinium* cf. *aureolum* or *Gymnodinium* cf. *nagasakiense*) which occur from the Atlantic to the English Channel (Partensky et al., 1991). Several works have been achieved in these areas in order to better understand the bloom dynamics of this species and subsequently build up mathematical models of this species (Morin et al., 1989; Gentien et al., 1997; Loyer et al., 2001; Vanhoutte-Brunier et al., 2008). The two most significant bloom events occurred in 1995 along the whole French Atlantic coast (Arzul et al., 1995) and in 2003 off the Western English Channel (Vanhoutte-Brunier et al., 2008). Massive mortality of marine fauna, including fish (wild and reared), sea urchins (*Echinocardium cordatum*), lugworms (*Arenicola marina*) and many bivalves was associated to the previous event (Arzul et al., 1995). The second one was intense and extended enough to be visible by remote sensing satellite of surface seawater color (Vanhoutte-Brunier et al., 2008). At a smaller scale, the Mediterranean coast and especially some lagoons, can also be affected by blooms of *Karenia mikimotoi*. In the Corsican lagoon of Diana, mortality of sea bass and sea bream, reared in cages, has already been reported (Bodennec et al., 1994). In 1994, in this same lagoon, another species first identified as *Gyrodinium corsicum* (Paulmier et al., 1995) and later transferred to the genus *Karlodinium* on the basis of its morphological similarities with other *Karlodinium* species (Siano et al., 2009), was responsible for a green discoloration of water. Farmed fish mortality was also observed but the toxicity of this dinoflagellate had not been demonstrated (Paulmier et al., 1995). Since that date, no bloom was recorded and the toxicity of this species could not be reconsidered. A third species, *Karenia papilionacea* Haywood et Steidinger (first identified as *Gymnodinium* cf. *breve*), has been observed in low abundance since 1994 especially in Western Brittany on the Atlantic coast (Nézan, 1998; Haywood et al., 2004). In the early 2000s, a study of the genetic diversity of the genus *Karenia* along the French coasts was achieved but did not reveal any other species than those previously identified (Guillou et al., 2002).

In 2008, massive losses of juvenile oysters along the French coasts brought back the attention towards the family Kareniaceae. A number of 58 water samples were collected in several production areas of oysters. Although this family was present in 39 samples, no bloom was observed and cultures which could have allowed the analysis

of the harmfulness of Kareniaceae were not established. Over a period of two years (2012-2013), single cells of Kareniaceae were isolated from live material sampled on both Atlantic (Brittany) and Mediterranean (Corsica) coasts in order to start cultures and evaluate their potential toxicity. Several strains were thus obtained, including a novel *Karlodinium* species. In this paper, we first analyze all data (partial rDNA sequences and images acquired from single cells and cultures) collected on Kareniaceae in France in order to contribute to the knowledge of the diversity and global biogeography of this family. Then, on the basis of one cultivated strain, we propose the description of a new species, *Karlodinium gentienii* sp. nov., using light and electron microscopy, molecular phylogeny, pigment composition and haemolytic activity.

2. Material and methods

2.1. Specimen collection and cultivation.

For specimen collection, a number of 19 near surface seawater samples collected between 2007 and 2013 in ten sites (5 from the Atlantic and 5 from Mediterranean Sea) by the IFREMER national monitoring network (REPHY) were selected for this study, based on the presence of Kareniaceae. They were either living or preserved with acidic Lugol's Iodine solution (0.1 % final concentration) and stored at 4 °C until examination.

For cultivation, single cells were isolated from live samples by micropipeting under an IMT2 inverted light microscope (Olympus, Tokyo, Japan) and placed on 96 well plates filled with 0.2 mL of K/2 medium (Keller et al., 1987). The plates were incubated at 16 °C under 80-100 $\mu\text{mol photons m}^{-2} \text{s}^{-1}$ in a 12:12 light:dark photoperiod. After some cell divisions, the clonal strains were transferred to plates with progressively increasing well volumes. Using this procedure, a clonal culture of *Karlodinium gentienii* sp. nov. was obtained. The strain was maintained in 50mL culture flasks and cultivated in the conditions described above. The corresponding seawater sample was collected in Concarneau Bay (47°50.091'N, 3°57.0369'W) in July 2012 when surface water temperature was 16.1 °C and salinity 34.9.

2.2. Light microscopy (LM)

For the study of the genetic diversity of Kareniaceae, the observations of seawater samples were carried out using an Olympus IX70 inverted light microscope equipped with differential interference optics and a digital camera DP72 (Olympus, Tokyo, Japan). For the description of *Karlodinium gentienii* sp. nov., live cultivated cells were examined under a BX41 (Olympus, Tokyo, Japan) upright microscope equipped with both differential interference optics, an Osram mercury short arc HBO 100W lamp as light source for epifluorescence, and filtersets U-MWU2 for DAPI stain (excitation: BP330-385; beamsplitter: DM400; and emission: BA420) and U-MWIB2 for chlorophyll autofluorescence (excitation: BP460-490; beamsplitter: DM505; and emission: BA510IF). This equipment allowed to visualize the chloroplasts directly or the nuclei after staining with 4', 6-diamidino-2-phenylindole (DAPI). Light micrographs of both fixed and living cells were obtained using a digital camera DP72 (Olympus, Tokyo, Japan). Measurements of live cultivated cells of *Karlodinium gentienii* in their exponential growth phase were performed on LM digital micrographs using ImageJ software (Rasband, 1997–2006).

2.3. Scanning electron microscopy (SEM)

To better observe external morphological features of *Karlodinium gentienii*, two procedures with a different combination of fixatives were attempted. For the first method, cultivated cells were fixed with an equal volume of 4 % osmium tetroxide (2% final concentration) and 0.5 % glutaraldehyde (final concentration) for 1h at room temperature, before a first rinse in seawater and a second rinse in deionized water. In the second procedure, cells were fixed with 1 % acidic Lugol's solution and 1 % glutaraldehyde (final concentrations). Fixed cells were stored at 4 °C before dehydrating. Then, they were processed according to the methods described in Couté (2002) and Chomérat and Couté (2008). After gold-palladium coating, cells were observed with a Quanta 200 (FEI, Eindhoven, Netherlands) scanning electron microscope. SEM images are presented on a uniform background using Adobe Photoshop CS2 (V. 9.0.2, Adobe Systems, San Jose, CA, USA).

2.4. Transmission electron microscopy (TEM)

TEM was used for the analysis of *K. gentienii* cell ultrastructure. Samples were fixed for 5 hours in a fixative mix containing 4 % glutaraldehyde, 0.2 M sodium cacodylate buffer (pH 7.4) and, 0.25 M sucrose. Samples were then rinsed in a series of buffer solutions containing graded concentrations of sucrose and NaCl (from 0.25 M sucrose, 0.22 M NaCl in 0.2 M sodium cacodylate to 0.35 M NaCl in 0.2 M sodium cacodylate) and post-fixed for 1 hour at 4 °C in 1 % osmium tetroxide buffered in 0.2 M of sodium cacodylate and 0.33 M NaCl. After rinsing three times for 15 min in 0.35 M NaCl and 0.2 M sodium cacodylate, dehydration was carried out in a graded alcohol series (from 30 to 100 %). Finally, samples were embedded in Epon resin. Sections were performed using diamond knives on a ultracut UCT ultramicrotome (Leica Microsystems, Wetzlar, Germany) and after stained with 2 % uranyl acetate for 10 min and 2 % lead citrate for 3 min. Sections were mounted on grids and examined with a Jeol 1400 transmission electron microscope (Jeol, Tokyo, Japan).

2.5. Genetic analyses

Single cells were isolated from live or Lugol-fixed samples by micropipeting under an Olympus IX70 inverted light microscope, and deposited on a glass slide. They were observed at 600X magnification, photographed with an Olympus DP72 digital camera, and rinsed into several drops of double distilled water (Milli-Q water) before transfer to a 0.2 ml PCR tube containing 3 µl of Milli-Q water. PCR tubes were stored at -20 °C until direct PCR amplifications. For PCR, tubes were thawed and processed as described in Nézan et al. (2012). The nuclear markers LSU rDNA and the internal transcribed spacer region (ITS1-5.8S rDNA-ITS2) were amplified using the primers given in Nézan et al. (2012).

Sequences were assembled using BioEdit v. 7.0.9.0 software (Hall, 1999). A total of 39 LSU rDNA sequences and two ITS region sequences were generated in our laboratory to infer the phylogeny of the Kareniaceae. The first set of sequences was aligned together with 52 LSU sequences of the order Gymnodiniales retrieved from GenBank and the second one with 12 ITS sequences, using the multiple sequence alignment program MUSCLE v. 3.7 (Edgar, 2004). Each alignment was refined by eye. The two data matrices obtained (92 LSU rDNA sequences, 830 characters and 14 ITS region sequences, 784 characters) were analyzed by two methods of phylogenetic reconstruction: maximum likelihood (ML), using PhyML v 3.0 software (Guindon and Gascuel, 2003) and Bayesian inference (BI) using MrBayes v.3.1.2 (Ronquist and Huelsenbeck, 2003). The software jModeltest v 0.1.1 (Posada, 2008) was first used to

select the most suitable model of substitutions. The General-Time Reversible models (GTR+ Γ_8) and (GTR+I+ Γ_4) were chosen for the LSU and ITS markers respectively, as indicated by the Hierarchical Likelihood Ratio Tests (hLRTs), Akaike Information Criterion 1 (AIC1), Akaike Information Criterion 2 (AIC2) and Bayesian Information Criterion (BIC) tests implemented in jModeltest. Bootstrap values (support for branches) of trees were obtained after 1000 iterations in ML. For Bayesian inference, four Markov chains were run simultaneously for 2×10^6 generations with sampling every 100 generations. On the 2×10^4 trees obtained, the first 2000 were discarded (burn-in) and a consensus tree was constructed from the remaining trees. The posterior probabilities corresponding to the frequency with which a node is present in preserved trees, were calculated using a coupled Monte Carlo Metropolis approach - Markov Chain (MCMC).

2.6. Pairwise distances

The genetic pairwise distances (p -distances), based on the D1-D2 region of the LSU rDNA gene were estimated using MEGA5 software (Tamura et al., 2011). Several sequences of *Karenia*, *Karlodinium* and *Takayama* retrieved in Genbank and acquired in this study (Table S1) were aligned using Clustal W in MEGA5. The variability between individuals of the same species was estimated by the range (minimum and maximum values) of pairwise distances retrieved from the distance matrix. To estimate the average range of distances between species within each genus, all sequences were assigned to groups (species) in MEGA5 and 'between groups means' were computed. Minimum and maximum mean values were given for each of the three genera. The taxa which were not identified at species-level were excluded from this calculation since it was not possible to assign them certainly in one group. Their average distance to the closest identified taxon was calculated to evaluate whether they were likely new undescribed species (p -value > average among species within a genus) or a known species with slightly divergent sequences (p -value < average among individuals within a species).

2.7. Pigment analyses.

Volumes of 30 mL of culture of *Karlodinium gentienii* in exponential phase were supplemented with pluronic acid, pelleted by centrifugation at $8,000 \times g$, and the pellets were then frozen and stored at $-80 \text{ }^\circ\text{C}$ until further analysis. The pellets were resuspended in 500 μL 100% cold methanol and stored at $-20 \text{ }^\circ\text{C}$ for 1 hour. *Karlodinium* pigments were easy to extract as the cells immediately and completely collapsed in methanol. The suspension was then centrifuged at $20,000 \times g$ to ensure the removal of all particles and cell debris. The supernatant was then brought to 10% Milli-Q water to avoid peak distortion (Zapata and Garrido, 1991) and a volume of 100 μL of the pigment extract was immediately injected into an HPLC Hewlett-Packard HPLC 1100 Series system, equipped with a quaternary pump and diode array detector. Pigment separations were performed using a Waters Symmetry C_8 column ($150 \times 3 \times 4.6 \text{ mm}$, $3.5 \mu\text{m}$ particle size) according to procedures published elsewhere (Zapata et al., 2000; Six et al., 2005) at a flow rate of 1 mL min^{-1} . All sample preparations were made under subdued light. Chlorophylls and carotenoids were detected by their absorbance at 440 nm and identified by diode array spectroscopy. Pigments were identified and quantified using standards derived from macroalgae and phytoplankton cultures by preparative HPLC (Repeta and Bjørnland, 1997), using previously compiled extinction coefficients (Roy et al., 2011). For comparison, the strain RCC2539 of *K. veneficum* was analyzed in the same conditions.

2.8. Haemolytic assay

Haemolytic activity of the culture of *Karlodinium gentienii* was assessed using the procedure described by Arzul et al. (1994) and modified by Eschbach et al. (2001). Horse blood obtained from Labocéan (Quimper, France) was used and the erythrocyte solution prepared according to Arzul et al. (1994).

Cells concentrations in the culture of *K. gentienii* in stationary phase were estimated with a Fuchs-Rosenthal counting chamber under a BX41 upright microscope. As the concentrations were not high enough to perform the tests in triplicate, a volume of the culture was centrifuged at $8,00 \times g$ for 15 min to concentrate cells in a pellet. The supernatant was discarded and the pellet containing a known number of algal cells was resuspended in 13.5 mL of NaCl (0.16 M) so that three tubes containing 4.5 mL of the algal solution and 500 μL of the erythrocyte solution (50×10^6 cells L^{-1}) could be prepared. Hence, two algal concentrations (20×10^3 cells mL^{-1} and 70×10^3 cells mL^{-1}) were tested in triplicate. For comparison, three tubes with a concentration of 20×10^3 cells mL^{-1} of *Karlodinium armiger* (strain IFR-KAR-01D) were prepared in the same way. To measure the natural haemolysis of erythrocytes occurring without addition of any haemolytic substance, 500 μL of the erythrocyte solution were added to 4.5 mL of NaCl solution at 0.16 M. In contrast, to induce 100 % haemolysis (control) by osmotic stress, 500 μL of the erythrocyte solution were added to 4.5 mL of distilled water. A standard curve with increasing concentrations of erythrocytes was prepared according to Eschbach et al. (2001) in order to relate the absorbance with the percentage of haemolysis. The suspensions were incubated in the dark at room temperature for 90 min. After incubation, samples were centrifuged 10 min at $8,00 \times g$ to pellet the intact erythrocytes. The absorbance of the supernatant was measured at 414 nm with a UV-1650PC spectrophotometer (Shimadzu, Kyoto).

3. Results

3.1. Genetic diversity of Kareniaceae

Molecular analyses of LSU rDNA sequences of individual cells allowed to assign 12 taxonomic units to the known genera *Karenia*, *Karlodinium* and *Takayama*, whereas one taxon could not be affiliated to any described genus and thus was classified at the family-rank. (Fig. 1 and Table 1). Our ML topology of the LSU (D1-D2 region) is coherent with those previously described (de Salas et al., 2008; Siano et al., 2009) except for a new independent clade formed by the identical sequences of two specimens of the unidentified Kareniaceae. (Fig. 1O-P). This clade is basal to the clades of the genera *Takayama* and *Karlodinium*, and separates from the clade corresponding to the genus *Karenia* (Fig. 2). The ML tree inferred from an ITS region (ITS1-5.8S rDNA-ITS2) data matrix confirms the position of this clade with a well-supported node (90 LBS, 1.00 BPP), and including not only our taxon entitled Kareniaceae sp. but also the Dinophyceae sp. from Ross Sea for which ITS sequences were available unlike LSU sequences (Figs. 1N and 3).

Among the twelve taxonomic units assigned to a known genus, seven of them referred to *Karenia brevisulcata*, *K. mikimotoi*, *K. papilionacea*, *K. umbella*, *Karlodinium armiger*, *K. decipiens* and *K. veneficum*, based on a 100% similarity with reference sequences. The five others formed a sister taxon of a known species, and their sequences were distant from sequences of the type locality. So, they could not be identified at species-level on the basis of molecular analysis only. The genetic distances were estimated showing that the variability among species within a genus ranged from 2.9 % to 9.0 % in *Karenia*, from 2.0 % to 9.9 % in *Karlodinium*, and from 1.1 % to 4.0 % in *Takayama*

(Table 2). The variability among individuals (strains) of the same species ranged from 0 % to 1.6 % for *Karenia* species, from 0 % to 1.5 % for *Karlodinium* species, and was null for *Takayama* species, except for *T. acrotrocha* (Table 2). A first unidentified taxon of the genus *Karenia*, named *K. sp1*, and originating from the Atlantic Ocean was a sister taxon to *K. papilionacea* in the ML tree inferred from LSU rDNA (D1-D2) sequences with a well-supported node (87 LBS, 1.00 BPP) while the average distance between these two taxa was 2.9 % (Fig. 2 and Table 2). A second taxon of the same genus, named *Karenia sp2*, and originating from Mediterranean Sea or Corsica coast clustered with *K. umbella* with a high support (97 LBS, 0.99 BPP) while the *p*-distance between these two taxa was 1.2 %. For the genus *Karlodinium*, two sequences of one unidentified taxon from the Atlantic and Mediterranean Sea formed a sister clade to the reference sequence of *K. corrugatum* from Southern Ocean with a high support (96 LBS, 1.00 BPP), while the distance between the two taxa was 2.7 %. This corresponding taxon was designated *Karlodinium sp.* Another taxon of the same genus and originating from the Atlantic clustered with *K. ballantinum* and was erected as a new species (see description below). For the genus *Takayama*, two sequences originating from the Atlantic and classified as *Takayama sp.* diverged from 0.4 % with the closest related sequences of *T. tasmanica* from Australia (type locality), New Zealand and China Sea. (Table 2).

3.2. Characterization of *Karlodinium gentienii*

3.2.1. *Karlodinium gentienii* Nézan, Chomérat et Siano sp. nov. (Figs. 4-8)

Diagnosis: unarmored and small cells, ovoid in shape, 13.5-18.9 µm long and 11.5-16.8 µm wide, and almost circular in transverse section. Epicone conical with parallel and twisted furrows underlied by rows of micro-processes. Hypocone hemispherical. Cingulum displaced 25–31 % of the cell length. Sulcus extending onto the epicone, and with an intercingular tubular structure. Apical groove or carina linear to slightly curved with thick margins, and extending briefly onto the dorsal epicone. Ventral pore present. Nucleus large, primarily central and irregular in shape. Several elongated chloroplasts (5-7) at the cell periphery, and containing conical pyrenoids. Amphiesmal plug-like structures not detected. A conspicuous trichocyst system connected to external micro-processes.

Holotype: SEM stub IFR-13J7, prepared from strain IFR-KGE-01C, fixed to display the amphiesmal vesicles, deposited at the Centre of Excellence for Dinophytes Taxonomy (CEDiT) with the accession reference CEDiT2014H38. Fig. 6A-G.

Isotypes: cells from a formalin fixed sample (strain IFR-KGE-01C) deposited at the CEDiT (designation CEDiT2014I39).

Etymology: the species is named to honour Dr. Patrick Gentien, our dear missing colleague and collaborator who was deeply involved in international cooperation on harmful algae bloom research. His contribution in the ecology and oceanography of *Karenia mikimotoi* was fundamental (Reguera and Smayda, 2012). This new *Karlodinium* species has been detected for the first time in 2010 in Brest Bay where Patrick spent many years of his professional career.

Type locality: Concarneau Bay (47°50.091'N, 3°57.0369'W).

Distribution: presently known from the Atlantic coast of Brittany.

Habitat and ecology: every time the organism has been detected in coastal plankton in late spring when water temperature reached 15-16 °C.

3.2.2. Species description

Karlodinium gentienii is a nanoplanktonic and unarmored dinoflagellate. It is small-sized with an average length of $16.3 \pm 1.5 \mu\text{m}$ (range 13.5–18.9 μm) and an average width of $13.6 \pm 1.4 \mu\text{m}$ (range 11.5–16.8 μm) ($n=30$). The median length to width ratio is 1.20.

Light microscopy (LM): cells appear ovoid in outline (Fig. 4A-B), and barely flattened dorsoventrally. The epicone is conical in shape with the apical groove and the ventral pore at times discernible (Fig. 4A). The hypocone is hemispherical, not truncated by the sulcus. The cingulum is excavated and left-handed (Fig. 4B-C). The sulcus is wide (Fig. 4C). The nucleus is large, irregular in shape and is normally located in the approximate center of the cell (Fig. 4B, F). The chloroplasts (5-7) are yellow-green in colour (Fig. 4D), variable in shape (Fig. 4D, E-F), and distributed at the cell periphery. Refractive bodies are present (Fig. 4A, D).

Regarding the swimming behaviour, cells progress at moderate speed in a straight undulating line. Sometimes, they slow down to continue or change direction.

Scanning electron microscopy (SEM): using the first method of cell fixation based on osmium tetroxide as first fixative, SEM allowed to describe in more detail the external morphology of the cells observed in LM (Fig. 5A-F). The cingulum is displaced 25–31 % of the cell length (Fig. 5A). The sulcus extends from just above the antapex to the proximal end of the cingulum (Fig. 5A). It is wide in the hypocone with a pronounced left curvature at the level of the insertion of the longitudinal flagellum (Fig. 5F). It becomes narrower in the intercingular region where a tube-shaped structure between the two flagellar pores is present (Fig. 5F). Then, it invades slightly the epicone as a finger-like protusion, with a prominent right margin in the epicone (Fig. 5F). The apical groove is directed obliquely, starting ventrally above the anterior end of the sulcus and ending dorsally in the upper sixth of the epicone (Fig. 5A-C, E). It is linear to slightly curved and 0.3 μm wide (Fig. 5C, E). An elongate ventral pore (0.8-1.0 μm in length) is present in the epicone, above the sulcal intrusion and close to the base of the apical groove (Fig. 5A, C).

When the membranous material or mucilage that covers the cell completely disappeared thanks to the second method of cell fixation using both a Lugol's solution and glutaraldehyde as fixatives, fine details of the cell surface are evident (Fig. 6A-G). The anterior side of the cingulum is delineated from the epicone by a list while its posterior border extends smoothly into the hypocone (Fig. 6A, C). The apical groove appears deep with thick margins (Fig. 6E). The amphiesmal vesicles, polygonal in shape, appear clearly all over on the cell, arranged in more or less distinct horizontal series (Fig. 6A-C). They are pentagonal or hexagonal except in the cingulum and along the apical groove where they tend to become quadrangular (Fig. 6F-G). They are arranged in 6 series on the epicone, 5 series on both the hypocone and the cingulum while the apical groove is lined on each side by one series. The surface of the epicone displays parallel furrows with tangential rows of rounded structures (number ca. 25 in 10 μm and 150 nm in diameter) close to the crests (Fig. 6A, C-D). These arrangements are twisted in relation to the cell longitudinal axis. Below the cingulum, the surface displays two parallel rows of pustular micro-processes (*sensu* Paulmier et al., 1995) or two striae of knobs (*sensu* Siano et al., 2009), the upper one being just below the cingular edge and the second one ca. 1.5 μm below (Fig. 6A, C, F).

Transmission electron microscopy (TEM): the ultrastructure of the cells observed on the basis of cell sections shows that the nucleus occupies a large space in the cell, although it was not always well preserved by fixation (Fig. 7A-B). It is centrally located, extending into the epicone, as shown in LM (Fig. 4B, F). In some specimens, it appears to extend into the hypocone (Fig. 7A), probably when the cell is dividing. The chloroplasts contain 1-2 pyrenoids, putatively conical in shape since they appear lenticular when observed in longitudinal section (Fig. 7D) and triangular in cross section (Fig. 7E). In the amphiesma, the apical groove and the cingulum are apparent in longitudinal sections (Fig. 7A-B). Amphiesmal vesicles are not visible neither in longitudinal sections nor in cross sections, probably due to methods of fixation used for TEM. A semi-opaque material is present beneath the outer membrane, interrupted by lipidic droplets (Fig. 8F). Bundles of parallel microtubules are present in tangential sections through the cell surface (Fig. 8G). Plug-like structures were never observed after examinations of many cell sections. A conspicuous trichocyst system is revealed in all cell sections (Figs. 7A-C and 8A-G). It is particularly developed in the epicone, over the nucleus and, to a lesser extent in the hypocone, close to the cingulum (Fig. 7A-B). The trichocysts are contained in long tubular cisternae that extend from the inner part of the cell towards the cell membrane (Figs. 7C and 8B). In their proximal part, the cisternae are filled with dense material surrounded by a double-membrane opaque wall (Fig. 8E). In the distal part of the cisternae, the trichocysts detach from the wall assuming a quadrangular shape (Fig. 8C). Lid-like structures cover the trichocyst exits (Fig. 8D) which are raised when the trichocysts are discharged (Figs. 7C and 8E). The number and the size of the lids (approximately 25 in 10 μm and 150 nm in diameter respectively) match those of the rounded structures observed in SEM. A conspicuous pusule system is associated to the flagellar apparatus (Fig. 7F-G). It is composed of tubes of two main size classes (approximately 0.2 μm and 0.08 μm in diameter); the larger tubes have a bright appearing lumen and a very thin external layer of dark material, conversely smaller tubes have a darker lumen (Fig. 7F-G). The flagellar apparatus was not integrally visible in our preparations, only one flagellar base and a striated root, likely *r4* (*sensu* Bergholtz et al., 2005), is clearly visible.

3.2.3. Phylogeny of *Karlodinium gentienii*

Phylogenetic analysis using ML methods (Fig. 2) showed that sequences of *Karlodinium gentienii* (from natural sample and culture) formed a well-supported independent clade (100 LBS, 1.00 BPP), clustering with *K. ballatinum* and the unspecified *Karlodinium* from Korea (strain KAMS0708), with high support (100 LBS, 1.00 BPP). The estimated genetic distances between *K. gentienii* and its closest related *K. ballatinum* and *K. sp.* from Korea were 2.8% and 2.7% respectively while the average among the species of *Karlodinium* ranged from 2.0% to 9.9% (Table 2).

3.2.4. Pigment profile

HPLC analyses of an autotrophically grown culture of *Karlodinium gentienii* revealed the presence of major pigments typical of fucoxanthin containing dinoflagellates with chloroplast Type 3, as described by Zapata et al. (2012) (Fig. 9). The results showed that *Karlodinium gentienii* contains chl c_2 and c_3 . The major carotenoid was fucoxanthin, along with moderate amounts of the two derivatives 19'-butanoyloxyfucoxanthin and 19'-hexanoyloxyfucoxanthin. A xanthophyll exhibiting similar absorption properties to an acyl-fucoxanthin compound eluted at 23 min. The photoprotective diadinoxanthin and diatoxanthin were also detected in significant amounts, as well as an unknown xanthophyll absorbing maximally at 442 nm and eluting at 19 min. No gyroxanthin-diester or gyroxanthin-like pigments and non polar-chl c_2 were detected.

3.2.5. Haemolytic activity

The preliminary assays showed that *Karlodinium gentienii* had a haemolytic activity. With a cell concentration of 20×10^3 cells mL⁻¹, an haemolysis of 2 % was found with *Karlodinium gentienii* while 40 % of the erythrocytes were lysed with *Karlodinium armiger*. A second analysis with a concentration of 70×10^3 cells mL⁻¹ of *K. gentienii* showed a lysis of 80 % of the erythrocytes.

4. Discussion

4.1.1. Genetic diversity of Kareniaceae

The molecular phylogenetic approach revealed a notable diversity of Kareniaceae in France including 13 taxonomic units. The unidentified Kareniaceae from the Atlantic (Fig. 1N-P) occupied the same phylogenetic position in our two ML trees (Figs. 2-3). It was distant from *Karlodinium antarcticum* (Fig. 2) and clustered with the Dinophyceae sp. from Ross Sea (Fig. 3). On this basis, we consider that the French unidentified Kareniaceae, together with the Dinophyceae sp. from Ross Sea, is distinct from *K. antarcticum* in spite of their resemblance as emphasized by de Salas et al. (2008) for the Dinophyceae sp. from Antarctica. According to our data, they likely belong to a novel genus, as already suggested by Gast et al. (2006). However, more data are needed before deciding conspecificity or discrimination between these two taxa.

Our survey confirmed the presence of *Karenia mikimotoi* and *K. papilionacea* on the French Atlantic coast and revealed for the first time the presence of both *K. brevisulcata*, previously recorded as *Gymnodinium brevisulcatum* (Chang, 1999) and *K. umbella* (de Salas et al., 2004). The latter two species have been described in New Zealand and Australia respectively, and do not seem to have been reported elsewhere. For the genus *Karlodinium*, *K. decipiens* was genetically detected in the Atlantic while the two potentially ichthyologic species *K. armiger* and *K. veneficum* were in both the Atlantic and Corsica. If *K. veneficum* is distributed worldwide, *K. decipiens* was reported only in Australian and Spanish Atlantic waters before and *K. armiger* was only known from the type locality Alfacs Bay (Spain) in NW Mediterranean.

The remaining taxa could not be identified at species-level, except for the sister taxon of *K. ballantinum* described in this paper. Concerning *Karenia* sp1 (Fig. 1G), the sister taxon of *K. papilionacea*, the branch length and the pairwise genetic distance between these two taxa (Fig. 2 and Table 2) seem to argue in favour of two distinct species unlike *Karenia* sp2 (Fig. 1E-F) which could be conspecific with *K. umbella*. Indeed, the *p*-distance between the two latter taxa was less than the maximum value of the interspecific variability between individuals of a same species. In order to resolve this taxonomic issue, a SEM examination of the Corsican strain of *Karenia* sp2 would be necessary to search for the characteristic furrows of *K. umbella*. As to *Karlodinium* sp. (Fig. 1L), the sister taxon to *K. corrugatum*, the sequence divergence between these two taxa was higher than the minimum value of the interspecific variability between *Karlodinium* species, suggesting separate species. However, further genetic and morphological investigations relative to these three unidentified Kareniaceae species are needed to assert all these assumptions. Finally, regarding the taxon *Takayama* sp. (Fig. 1M), the closest related to *T. tasmanica*, the genetic distance between these two taxa was low (0.4 %), which could mean that they were conspecific. However, De Salas et al. (2008) pointed out some variability in the same order of magnitude between species within the genus *Takayama*. In addition, Gu et al. (2013) indicated that the LSU rDNA gene may be too conservative in this genus, as in other

dinoflagellate groups. As a consequence, the French *Takayama* species was considered as unidentified until additional genetic and morphological data.

4.2. Characterization of *Karlodinium gentienii*

4.2.1. Morphological and genetic comparisons

Karlodinium gentienii was separated from the other species of *Karlodinium*, based on morphology, molecular phylogeny, and genetic data (Tables 2 and 3 and Fig. 2).

Morphological differences exist between *K. gentienii* and the other described *Karlodinium* species (Table 3). At the surface of the epicone of *K. gentienii*, the set of parallel spiral furrows was similar to that described for *K. corrugatum*. However, the location of the ventral pore well away from the sulcus distinguishes *K. corrugatum* (de Salas et al., 2008) from the new species. In addition, rounded episomic structures were aligned along the furrows in *K. gentienii* unlike in *K. armiger* where they are randomly placed (Bergholtz et al., 2005). These structures were also observed as two parallel rows below the cingulum of *K. gentienii* like *K. corsicum* (Paulmier et al., 1995). However, these two taxa differed in the cell length, the girdle displacement, the number and the color of chloroplasts. And, the micro-pustules arranged in two longitudinal rows in the cingulum as described by Paulmier et al. (1995) for *K. corsicum* were not observed in the new species. Another species *K. ballatinum* was also described with two rows of rounded structures (striae of knobs) but a single row was hyposomic, the other one being episomic (de Salas et al., 2008; Siano et al., 2009). The intercingular tube-shaped structure in the sulcus of *K. gentienii* has also been reported in *K. australe* (de Salas et al., 2005) and *K. ballatinum* (de Salas et al., 2008) and may be homologous with the putative “platelet” of *K. corsicum* (Paulmier et al., 1995) or peduncle of *K. veneficum* (Taylor, 1992). This structure is common to the species of *Karenia* and *Takayama* (Haywood et al., 2004; Gu et al., 2013) and has been also observed in *Asterodinium gracile*, a putative member of the Kareniaceae together with *Brachidinium capitatum* (Gómez et al., 2005; Henrichs et al., 2011). Accordingly, this character might be common to all species of Kareniaceae, as suggested by Haywood et al. (2004). The arrays of plug-like structures immediately below the amphiesma have not been observed in *K. gentienii*, despite many cell sections. Considering that cells lost most of the amphiesma when fixed for TEM, it is difficult to determine on the presence or absence of plug-like structures. Dischargeable trichocysts were particularly numerous both in the epicone and below the cingulum of *K. gentienii* in contrast to *K. armiger* where they are limited to the epicone (Bergholtz et al., 2005). Interestingly, both the lids of the trichocyst-containing cisternae and the external micro-structures were similar in number and size in *K. gentienii*, suggesting that the arrays of trichocysts observed in TEM match the rows of micro-processes observed on the cell surface in SEM. This correspondence was made possible thanks to the clear visualization of micro-processes, using a suitable preservation method to remove the outer membrane of the cells.

The phylogenetic position of *K. gentienii* together with *K. ballatinum* and *K. sp.* from Korea in a strongly supported clade and the pairwise distances between *K. gentienii* and its two sister taxa support also the erection of *K. gentienii* as a new species.

4.2.2. Pigment composition

The pigmentation of only four species of *Karlodinium* has been described to date and the variable part of the pigmentation among these species seems to rely mostly on the

presence/absence of gyroxanthin derivatives and non polar-chl c_2 compounds. All analyzed strains of the most studied species, *K. veneficum*, contain gyroxanthin esters in significant amounts and no non polar-chl c_2 (Kempton et al., 2002; Garcés et al., 2006; Bachvaroff et al., 2009; Zapata et al., 2012) (Table S2). By contrast, the strain of *K. australe* analyzed by de Salas et al. (2005) did not synthesize any gyroxanthin derivative but did contain non polar-chl c_2 eluting after chl *a*. In *K. armiger* and *K. decipiens* strains, both pigments are usually present (Bergholtz et al., 2005; Garcés et al., 2006; Zapata et al., 2012). The novel species described here, *Karlodinium gentienii*, contained neither gyroxanthin derivatives nor non polar-chl c_2 compounds and thus shows a new combination of pigments in the *Karlodinium* genus.

4.2.3. Haemolytic activity

Although a haemolytic activity has been found with *Karlodinium gentienii*, it appears lower than with *K. armiger*, which has been proven to be ichthyologic (Garcés et al., 2006). Nevertheless, further analyses are necessary to measure comparatively with more cells concentrations, and investigate several other strains and species.

5. Conclusions

Even though one genus and several species remain to be identified, requiring new attempts of cultivation, this study strengthens our knowledge of the diversity of Kareniaceae in France, with the certainty of a novel genus and the description of a new potentially toxic species: *Karlodinium gentienii*. Future works should focus on the geographic distribution of Kareniaceae species and, especially the new potentially toxic species *K. gentienii*, by further investigating the waters from the English Channel and the Mediterranean Sea. Pigment analyses showed that gyroxanthin and non polar chl c_2 compounds appeared to constitute a relevant criterion for the delineation of *Karlodinium* species. It would therefore be worth exploring the pigmentation of the other *Karlodinium* species in detail in the future. At last, characterization of haemolytic compounds and toxins should be undertaken in order to assess the potential risks induced by *Karlodinium gentienii* in the field.

Acknowledgements

We are grateful to Yoann Baldi for providing Corsican samples. Thanks to Evelyne Erard-Le Denn who isolated *Karenia mikimotoi* for culturing (strain GATIN95), and Laureline Le Montagner who isolated *K. mikimotoi* and *K. umbella* from Saint Pierre and Miquelon for molecular analysis (GenBank accession numbers KJ508364 and KJ508372). The Roscoff Culture Collection is warmly thanked for the maintenance of the *Karlodinium veneficum* strain RCC2539, as well as S. Ota who isolated it. Financial support was provided by IFREMER through the project DIALTOXE (Diversité algale, efflorescences toxiques, eutrophisation).

References

- Arzul, G., Gentien, P., Crassous, M.-P., 1994. A haemolytic test to assay toxins excreted by the marine dinoflagellate *Gyrodinium* cf. *aureolum*. *Water Research* 28(4), 961-965.
- Arzul, G., Belin, C., Nézan, E., 1995. Ichthyotoxic events associated with *Gymnodinium* cf. *nagasakiense* on the Atlantic coast of France. *Harmful Algae News* 12-13, 8-9.
- Bachvaroff, T.R., Adolf, J.E., Place, A.R., 2009. Strain variation in *Karlodinium veneficum* (Dinophyceae): Toxin profiles, pigments, and growth characteristics. *J. Phycol.* 45(1), 137-153.
- Bergholtz, T., Daugbjerg, N., Moestrup, Ø., Fernández-Tejedor, M., 2005. On the identity of *Karlodinium veneficum* and description of *Karlodinium armiger* sp. nov. (Dinophyceae), based on light and electron microscopy, nuclear-encoded LSU rDNA, and pigment composition. *J. Phycol.* 42, 170-193.
- Bodennec, G., Arzul, G., Erard le Denn, E., Gentien, P., 1994. *Gymnodinium* sp. dans l'étang de Diane (Corse) septembre - octobre 1993. Tests biologiques et analyses chimiques. DEL/94.07/Brest. Ifremer, Brest, p. 26.
- Chang, F.H., 1999. *Gymnodinium brevisulcatum* sp. nov. (Gymnodiniales, Dinophyceae), a new species isolated from the 1998 summer toxic bloom in Wellington Harbor, New Zealand. *Phycologia* 38, 377-384.
- Chomérat, N., Couté, A., 2008. *Protoperidinium bolmonense* sp. nov. (Peridinales, Dinophyceae), a small dinoflagellate from a brackish hypereutrophic lagoon (South of France). *Phycologia* 47(4), 392-403.
- Clément, A., Seguel, M., Arzul, G., Guzmán, L., Alarcon, C., 2001. Widespread outbreak of a haemolytic, ichthyotoxic *Gymnodinium* sp. in Southern Chile, In: Hallegraeff, G.M., Blackburn, S.I., Bolch, C.J., Lewis, R.J. (Eds.), Ninth International Conference on Harmful Algal Blooms, 7-11 February 2000, Hobart, Australia. International Oceanographic Commission of UNESCO, Paris, pp. 66-69.
- Couté, A., 2002. Biologie et microscopie électronique à balayage. *Mémoires de la SEF* 6, 31-44.
- Dahl, E., Tangen, K., 1993. 25 years experience with *Gyrodinium aureolum* in Norwegian waters, In: Smayda, T.J., Shimizu, Y. (Eds.), Toxic phytoplankton blooms in the Sea. Elsevier Science Publishers, B.V., Amsterdam, pp. 15-21.
- Daugbjerg, N., Hansen, G., Larsen, J., Moestrup, Ø., 2000. Phylogeny of some of the major genera of dinoflagellates based on ultrastructure and partial LSU rDNA sequence data, including the erection of three new genera of unarmoured dinoflagellates. *Phycologia* 39(4), 302-317.
- de Salas, M., Bolch, C.J., Botes, L., Nash, G., Wright, S.W., Hallegraeff, G., 2003. *Takayama* gen. nov. (Gymnodiniales, Dinophyceae), a new genus of unarmored dinoflagellates with sigmoid apical grooves, including the description of two new species. *J. Phycol.* 39, 1233-1246.
- de Salas, M., Bolch, C., Hallegraeff, G., 2004. *Karenia umbella* sp. nov. (Gymnodiniales, Dinophyceae), a new potentially ichthyotoxic dinoflagellate species from Tasmania, Australia. *Phycologia* 43(2), 166-175.

- de Salas, M., Bolch, C.J., Hallegraef, G., 2005. *Karlodinium australe* sp. nov. (Gymnodiniales, Dinophyceae), a new potentially ichthyotoxic unarmoured dinoflagellate from lagoonal habitats of south-eastern Australia. *Phycologia* 44(6), 640-650.
- de Salas, M., Laza-Martínez, A., Hallegraef, G., 2008. Novel unarmoured dinoflagellates from the toxigenic family Kareniaceae (Gymnodiniales): five new species of *Karlodinium* and one new *Takayama* from the Australian sector of the Southern Ocean. *J. Phycol.* 44, 241-257.
- Deeds, J.R., Terlizzi, D.E., Adolf, J.E., Stoecker, D.K., Place, A.R., 2002. Toxic activity from cultures of *Karlodinium micrum* (= *Gyrodinium galatheanum*) (Dinophyceae) - a dinoflagellate associated with fish mortalities in an estuarine aquaculture facility. *Harmful Algae* 1, 169-189.
- Edgar, R.C., 2004. MUSCLE: a multiple sequence alignment method with reduced time and space complexity. *BMC Bioinformatics* 5, 113.
- Eschbach, E., Scharsack, J.P., John, U., Medlin, L.K., 2001. Improved erythrocyte lysis assay in microtitre plates for sensitive detection and efficient measurement of haemolytic compounds from ichthyotoxic algae. *Journal of applied toxicology : JAT* 21(6), 513-519.
- Garcés, E., Fernandez, M., Penna, A., van Lenning, K., Gutierrez, A., Camp, J., Zapata, M., 2006. Characterization of NW Mediterranean *Karlodinium* spp. (Dinophyceae) strains using morphological, molecular, chemical, and physiological methodologies. *J. Phycol.* 42, 1096-1112.
- Gast, R.J., Moran, D.M., Beaudoin, D.J., Blythe, J.N., Dennett, M.R., Caron, D.A., 2006. Abundance of a novel dinoflagellate phylotype in the Ross Sea, Antarctica. *J. Phycol.* 42, 233-242.
- Gentien, P., Lazure, P., Raffin, B., 1998. Effect of meteorological conditions in spring on the extent of a *Gymnodinium* cf. *nagasakiense* bloom, In: Reguera, B., Blanco, J., Fernández, M.L., Wyatt, T. (Eds.), 8th International Conference on Harmful Algae. Xunta de Galicia and Intergovernmental Oceanographic Commission of UNESCO, Paris.
- Gómez, F., Nagahama, Y., Takayama, H., Furuya, K., 2005. Is *Karenia* a synonym of *Asterodinium-Brachidinium* (Gymnodiniales, Dinophyceae)? *Acta Bot. Croat.* 64(2), 263-274.
- Gu, H., Luo, Z., Zhang, X., Xu, B., Fang, Q., 2013. Morphology, ultrastructure and phylogeny of *Takayama xiamenensis* sp. nov. (Gymnodiniales, Dinophyceae) from the East China Sea. *Phycologia* 52(3), 256-265.
- Guillou, L., Nézan, E., Cuff, V., Erard-Le Denn, E., Cambon-Bonavita, M.A., Gentien, P., Barbier, G., 2002. Genetic diversity and molecular detection of three toxic dinoflagellate genera (*Alexandrium*, *Dinophysis*, and *Karenia*) from French coasts. *Protist* 153(3), 223-238.
- Guindon, S., Gascuel, O., 2003. A simple, fast, and accurate algorithm to estimate large phylogenies by maximum likelihood. *Syst. Biol.* 52(5), 696-704.

Hall, T.A., 1999. BioEdit: a user-friendly biological sequence alignment editor and analysis program for Windows 95/98/NT. *Nucleic Acids Symp. Ser.* 41, 95-98.

Hallegraeff, G.M., 2002. *Aquaculturists' guide to harmful Australian microalgae*. Print Centre, Hobart, Australia.

Hallegraeff, G.M., Mooney, B., Evans, K., 2010. What triggers fish-killing *Karlodinium veneficum* dinoflagellate blooms in the Swan Canning River system? Final report SRT project no. RSG09TAS01. Swan Canning Research and Innovation Program, pp. 1-30.

Haywood, A.J., Steidinger, K.A., Truby, E.W., 2004. Comparative morphology and molecular phylogenetic analysis of three new species of the genus *Karenia* (Dinophyceae) from New Zealand. *J. Phycol.* 40, 165-179.

Henrichs, D.W., Sosik, H.M., Olson, R.J., Campbell, L., 2011. Phylogenetic analysis of *Brachidinium capitatum* (Dinophyceae) from the Gulf of Mexico indicates membership in the Kareniaceae. *J. Phycol.* 47, 366-374.

Keller, M.D., Selvin, R.C., Claus, W., Guillard, R.R.L., 1987. Media for the culture of oceanic ultraphytoplankton. *J. Phycol.* 23, 633-638.

Kempton, J.W., Lewitus, A.J., Deeds, J.R., McHugh Law, J., Place, A.R., 2002. Toxicity of *Karlodinium micrum* (Dinophyceae) associated with a fish kill in a South Carolina brackish retention pond. *Harmful Algae* 1, 233-241.

Landsberg, J.H., Steidinger, K.A., 1998. A historical review of *Gymnodinium breve* red tides implicated in mass mortalities of the manatee (*Trichechus manatus latirostris*) in Florida, USA., In: Reguera, B., Blanco, J., Fernández, M.L., Wyatt, T. (Eds.), *Proceedings of the VIII International conference on Harmful Algae*, Vigo, Spain, 25-29 June 1997. Xunta de Galicia and Intergovernmental Oceanographic Commission of UNESCO, Paris, pp. 97-100.

Loyer, S., Lazure, P., Gentien, P., Menesguen, A., 2001. Modelling of *Gymnodinium mikimotoi* blooms along the French Atlantic coast: geographical and vertical distributions. *Hydroécologie Appliquée* 13(1), 57-76.

Medhioub, A., Medhioub, W., Amzil, Z., Sibat, M., Bardouil, M., Ben Neila, I., Mezghani, S., Hamza, A., Lassus, P., 2009. Influence of environmental parameters on *Karenia selliformis* toxin content in culture. *Cah. Biol. Mar.* 50, 333-342.

Morin, P., Birrien, J.-L., Le Corre, P., 1989. The frontal systems in the Iroise Sea: development of *Gyrodinium aureolum* Hulbert on the inner front. *Sci. Mar.* 53(2-3), 215-221.

Nézan, E., 1998. Recurrent observations of a *Gymnodinium breve*-like species. *Harmful Algae News* 17, 7.

Nézan, E., Tillmann, U., Bilien, G.I., Boulben, S., Chèze, K., Zentz, F., Salas, R., Chomérat, N., 2012. Taxonomic revision of the dinoflagellate *Amphidoma caudata*: Transfer to the genus *Azadinium* (Dinophyceae) and proposal of two varieties, based on morphological and molecular phylogenetic analyses. *J. Phycol.* 48(4), 925-939.

Partensky, F., Gentien, P., Sournia, A., 1991. *Gymnodinium* cf. *nagasakiense* = *Gyrodinium* cf. *aureolum* (Dinophycées), In: Sournia, A., Belin, C., Berland, B., Erard le Denn, E., Gentien, P., Grzebyk, D., Marcaillou le Baut, C., Lassus, P., Partensky, F.

(Eds.), Le phytoplancton nuisible des côtes de France : de la biologie à la prévention. CNRS - Ifremer, Plouzané, pp. 63-82.

Paulmier, G., Berland, B., Billard, C., Nézan, E., 1995. *Gyrodinium corsicum* nov. sp. (Gymnodiniales, Dinophycées), organisme responsable d'une "eau verte" dans l'étang marin de Diana (Corse) en avril 1994. *Cryptog. Algol.* 16(2), 77-94.

Place, A.R., Bowers, H.A., Bachvaroff, T.R., Adolf, J.E., Deeds, J.R., Sheng, J., 2012. *Karlodinium veneficum* — The little dinoflagellate with a big bite. *Harmful Algae* 14, 179-195.

Posada, D., 2008. jModelTest: Phylogenetic model averaging. *Mol. Biol. Evol.* 25(7), 1253-1256.

Rasband, W.S., 1997–2006. ImageJ, 1.37c ed. National Institutes of Health, Bethesda, Maryland.

Reguera, B., Smayda, T.J., 2012. In memoriam: Tribute to Patrick Gentien (29 November 1950–9 May 2010). *Harmful Algae* 14, 5-9.

Repeta, D.J., Bjørnland, T., 1997. Preparation of carotenoid standards, In: Jeffrey, S.W., Mantoura, R.F.C., Wright, S.W. (Eds.), *Phytoplankton pigments in oceanography: guidelines to modern methods*. UNESCO, Paris, pp. 239-260.

Ronquist, F., Huelsenbeck, J.P., 2003. MrBayes 3: Bayesian phylogenetic inference under mixed models. *Bioinformatics* 19(12), 1572-1574.

Roy, S., Llewellyn, C.A., Eglund, E.S., Johnsen, G., 2011. *Phytoplankton pigments, characterization, chemotaxonomy, and applications in oceanography*. Cambridge University Press, Cambridge, UK.

Siano, R., Kooistra, W.H.C.F., Montresor, M., Zingone, A., 2009. Unarmoured and thin-walled dinoflagellates from the Gulf of Naples, with the description of *Woloszynskia cincta* sp. nov. (Dinophyceae, Suessiales). *Phycologia* 48(1), 44-65.

Six, C., Worden, A.Z., Rodríguez, F., Moreau, H., Partensky, F., 2005. New insights into the nature and phylogeny of Prasinophyte antenna proteins: *Ostreococcus tauri*, a case study. *Mol. Biol. Evol.* 22(11), 2217-2230.

Takayama, H., Adachi, R., 1984. *Gymnodinium nagasakiense* sp. nov., a red tide forming dinophyte in the adjacent waters of Japan. *Bull. Plankton Soc. Jpn.* 31, 7-14.

Tamura, K., Peterson, D., Peterson, N., Stecher, G., Nei, M., Kumar, S., 2011. MEGA5: Molecular Evolutionary Genetics Analysis using Maximum Likelihood, evolutionary distance, and Maximum Parsimony methods. *Mol. Biol. Evol.* 28(10), 2731-2739.

Taylor, F.J.R., 1992. The taxonomy of harmful marine phytoplankton. *G. bot. ital.* 126, 209-219.

Vanhoutte-Brunier, A., Fernand, L., Ménesguen, A., Lyons, S., Gohin, F., Cugier, P., 2008. Modelling the *Karenia mikimotoi* bloom that occurred in the western English Channel during summer 2003. *Ecological Modelling* 210(4), 351-376.

Zapata, M., Garrido, J.L., 1991. Influence of injection conditions in reversed-phase high-performance liquid chromatography of chlorophylls and carotenoids. *Chromatographia* 31(11-12), 589-594.

Zapata, M., Rodríguez, F., Garrido, J.L., 2000. Separation of chlorophylls and carotenoids from marine phytoplankton: a new HPLC method using a reversed phase C₈ column and pyridinecontaining mobile phases. *Mar. Ecol. Prog. Ser.* 195, 29-45.

Zapata, M., Fraga, S., Rodríguez, F., Garrido, J.L., 2012. Pigment-based chloroplast types in dinoflagellates. *Mar. Ecol. Prog. Ser.* 465, 33-52.

Table 1. List of new sequence data from French specimens of Kareniaceae used for phylogenetic analysis. Area and date of collection, isolate and accession numbers are provided.

Taxon	Collection Area*	Collection date**	Isolate no.	GenBank no.
<i>Karenia brevisulcata</i>	Atlantic coast (47.837 N -3.950 W)	11 Aug. 2009 (17.3 °C)	IFR1133	KJ508359
<i>Karenia mikimotoi</i>	Mediterranean coast (43.456 N 4.497 W)	25 May 2009 (23.9 °C)	IFR980	KJ508361
	Atlantic coast (48.335 N -4.366 W)	18 Aug. 1995 (n. a.)	GATIN95	KJ508362
	Atlantic coast (47.837 N -3.950 W)	23 April 2008 (11.7 °C)	IFR559	KJ508363
<i>Karenia papilionacea</i>	Atlantic coast (48.163 N -4.392 W)	31 July 2007 (17.9 °C)	IFR562	KJ508366
<i>Karenia umbella</i>	Atlantic coast (48.163 N -4.392 W)	30 June 2008 (19.8 °C)	IFR644	KJ508368

<i>Karenia</i> sp1	Atlantic coast	31 July 2007	IFR528	KJ508373
	(48.163 N -4.392 W)	(17.9 °C)		
	Atlantic coast	19 June 2007	IFR572	KJ508374
	(47.837 N -3.950 W)	(16.6 °C)		
<i>Karenia</i> sp2	Mediterranean lagoon	23 April 2007	IFR868	KJ508369
	(42.872 N 3.014 W)	(20.2 °C)		
	Mediterranean lagoon	28 Oct. 2009	IFR1186	KJ508370
	(42.967 N 3.007 W)	(15.8 °C)		
	Corsican lagoon	13 May 2013	IFR-KUM-01U	KJ508371
	(42.046 N 9.478 W)	(22.7 °C)		
<i>Karlodinium armiger</i>	Corsican lagoon	27 May 2013	IFR-KAR-01D	KJ508375
	(42.128 N 9.529 W)	(19.4 °C)		
	Atlantic coast	14 June 2010	IFR10-093	KJ508376
	(48.163 N -4.392 W)	(15.6 °C)		
<i>Karlodinium decipiens</i>	Atlantic coast	07 June 2010	IFR10-069	KJ508377
	(48.335 N -4.366 W)	(15.5 °C)		

<i>Karlodinium gentienii</i>	Atlantic coast	07 June 2010	IFR10-074	KJ508378
	(48.335 N -4.366 W)	(15.5 °C)		
	Atlantic coast	02 July 2012	IFR-KGE-	KJ508379
	(47.837 N -3.950 W)	(16.1 °C)	01C	
<i>Karlodinium veneficum</i>	Atlantic coast	19 July 2010	IFR10-150	KJ508380
	(48.256 N -4.557 W)	(18.6 °C)		
	Corsican lagoon	27 May 2013	IFR-KVE-	KJ508381
	(42.128 N 9.529 W)	(19.4 °C)	01D	
	Atlantic coast	14 June 2010	IFR10-101	KJ508382
	(48.163 N -4.392 W)	(15.6 °C)		
<i>Karlodinium</i> sp.	Atlantic coast	15 July 2008	IFR797	KJ508385
	(48.163 N -4.392 W)	(18.9 °C)		
	Mediterranean coast	25 May 2009	IFR981	KJ508386
	(43.456 N 4.497 W)	(23.9 °C)		
<i>Takayama</i> sp.	Atlantic coast	23 June 2008	IFR863	KJ508387
	(47.535 N -3.094 W)	(16.6 °C)		
	Atlantic coast	23 June 2008	IFR909	KJ508388
	(47.535 N -3.094 W)	(16.6 °C)		

Kareniaceae sp.	Atlantic coast	20 April 2010	IFR11-001	KJ508389
	(47.837 N -3.950 W)	(11.7 °C)		
	Atlantic coast	20 April 2010	IFR11-015	KJ508390
	(47.837 N -3.950 W)	(11.7 °C)		
	Atlantic coast	20 April 2010	IFR10-474	KJ858681
	(47.837 N -3.950 W)	(11.7 °C)		

In brackets: * geographic coordinates, ** seawater temperature, n.a.: not available.

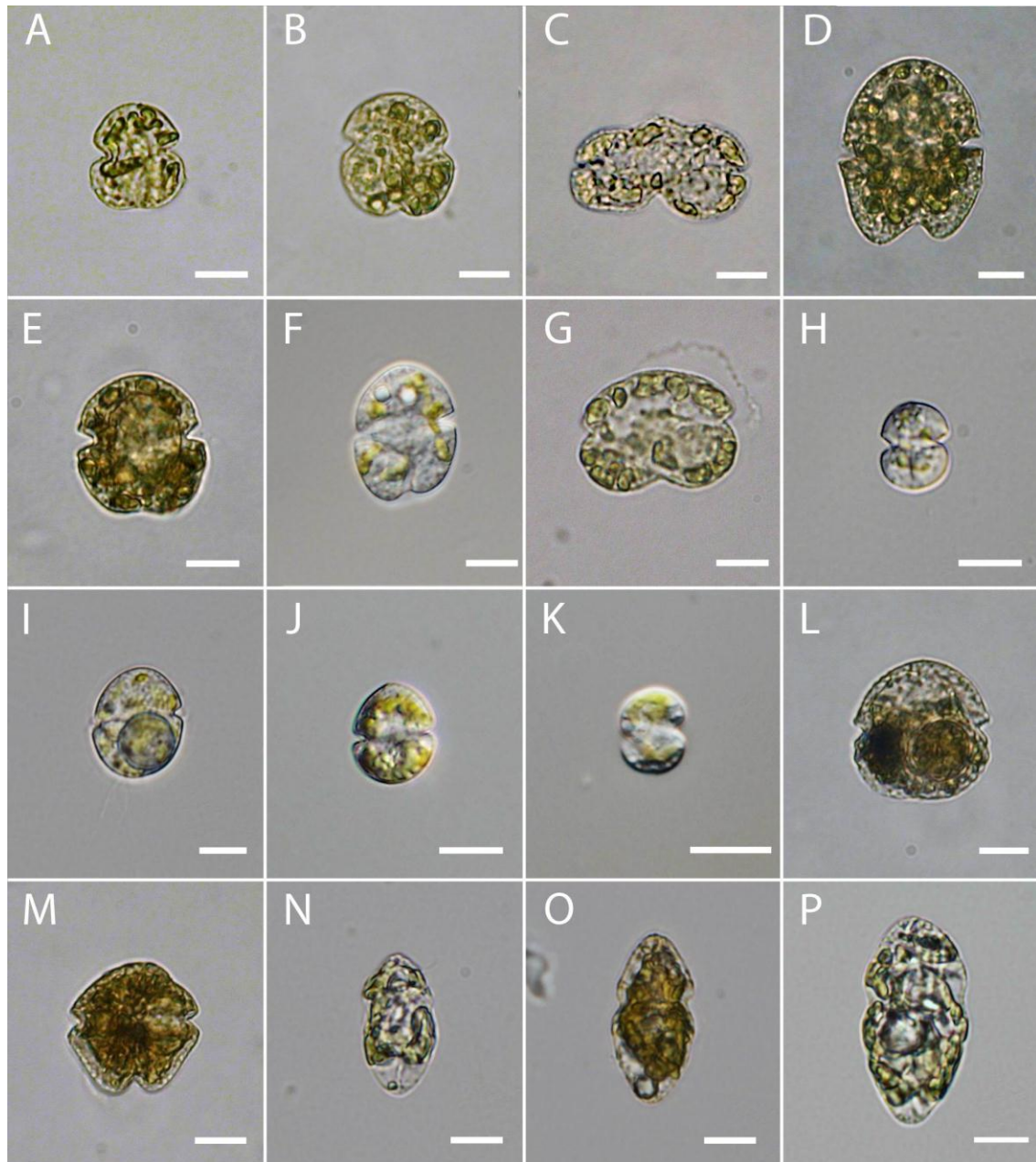


Fig. 1. Light micrographs of some specimens of Kareniaceae used for single-cell PCR analysis, with GenBank accession numbers in square brackets. (A) *Karenia brevisulcata* [KJ508359]. (B) *K. mikimotoi* [KJ508363]. (C) *K. papilionacea* [KJ508366]. (D) *K. umbella*. [KJ508368]. (E-F) *Karenia* sp2. (E) [KJ508370]. (F) [KJ508371]. (G) *Karenia* sp1. [KJ508373]. (H) *Karlodinium armiger* [KJ508375]. (I) *K. decipiens* [KJ508377]. (J) *K. gentienii* [KJ508379]. (K) *K. veneficum* [KJ508381]. (L) *Karlodinium* sp. [KJ508385]. (M) *Takayama* sp. [KJ508387]. (N-P) Kareniaceae sp. (N) [KJ858681]. (O) [KJ508389]. (P) [KJ508390]. Cells fixed with Lugol's solution (A-E, G, L-P). Live cells (F, H-K). Scale bars = 10 μ m.



Fig. 2. ML tree of the Kareniaceae (*Karenia*, *Karlodinium*, *Takayama*) inferred from a LSU rDNA (D1-D2 region) data matrix (92 sequences, 830 characters). The tree was rooted using *Alexandrium minutum* as outgroup. The General-Time Reversible model (GTR+ Γ_4) was chosen in jModeltest. Base frequencies were f(A) = 0.25358; f(C) = 0.21486; f(G) = 0.27066 and f(T) = 0.26091. Base substitutions rates were A \leftrightarrow C = 0.50398; A \leftrightarrow G = 1.17068; A \leftrightarrow T = 0.66736; C \leftrightarrow G = 0.79332; C \leftrightarrow T = 3.45783 against G \leftrightarrow T = 1. Rates at variable sites were assumed to be gamma distributed with the gamma shape parameter estimated to $\alpha = 0.4641$. Block dots corresponded to bootstrap values of 100 for Maximum Likelihood (ML) and posterior probabilities of 1.00 for Bayesian Inference (BI). Near each node were given bootstrap values of ML and posterior probabilities of BI respectively. If bootstrap values were < 65 and posterior probabilities < 0.85, the symbol "+" was used. The symbol "-" indicated an irresolution in the bayesian analysis. New sequences acquired in this study are shown in boldface. The taxa that could not be identified at species-level on the sole basis of molecular analysis are overlined in grey.

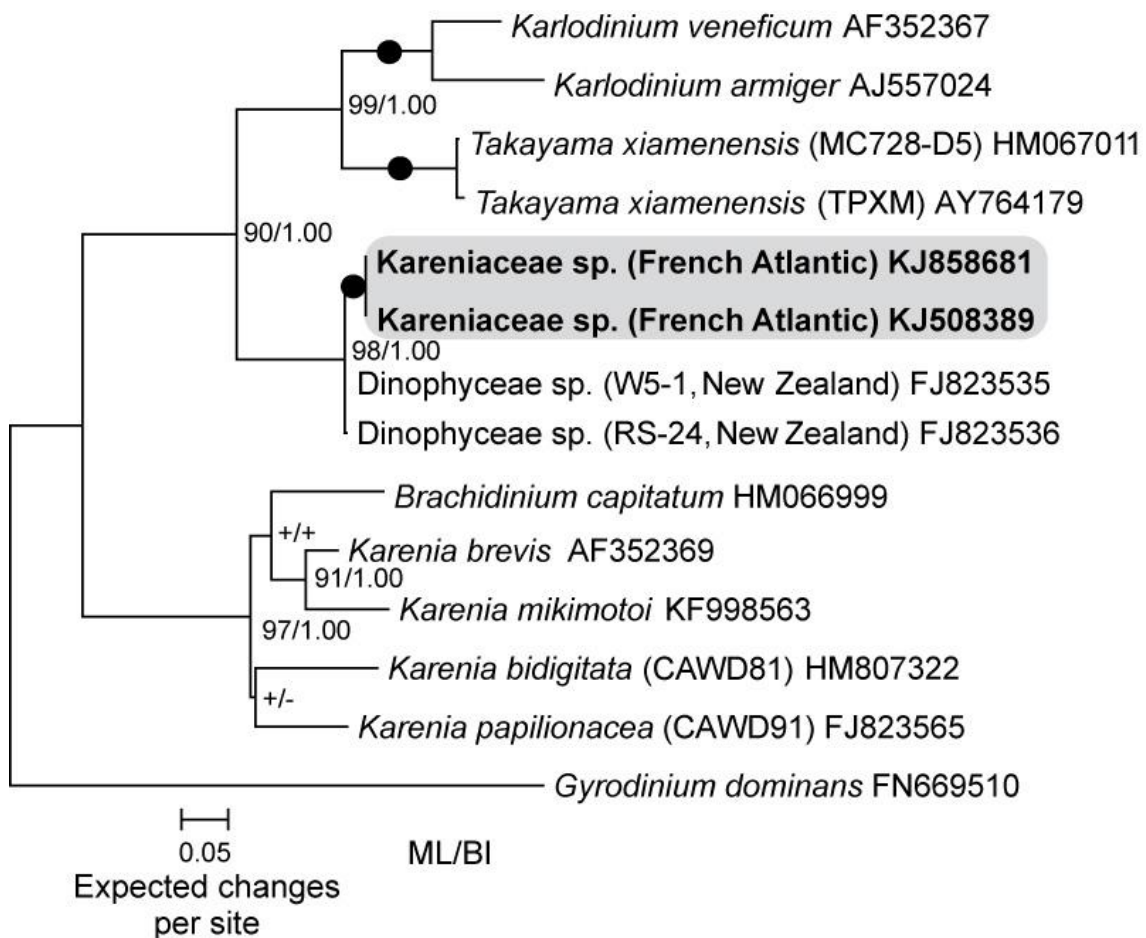


Fig. 3. ML tree of the unidentified kareniacean genus inferred from an ITS region (ITS1, 5.8S, and ITS2) data matrix (14 sequences and 784 characters). The tree was rooted using *Gyrodinium dominans* sequence as outgroup. The General-Time Reversible model (GTR+I+ Γ_4) was chosen in jModeltest. Base frequencies were $f(A) = 0.21769$; $f(C) = 0.23280$; $f(G) = 0.24615$ and $f(T) = 0.30335$. Base substitutions rates were $A \leftrightarrow C = 0.49822$; $A \leftrightarrow G = 1.27311$; $A \leftrightarrow T = 0.97504$; $C \leftrightarrow G = 0.45649$; $C \leftrightarrow T = 3.65847$ against $G \leftrightarrow T = 1$. Among-sites rate variation: assumed proportion of invariable sites = 0.214. Rates at variable sites were assumed to be gamma distributed with the gamma shape parameter estimated to $\alpha = 0.467$. Block dots corresponded to bootstrap values of 100 for Maximum Likelihood (ML) and posterior probabilities of 1.00 for Bayesian Inference (BI). Near each node were given bootstrap values of ML and posterior probabilities of BI respectively. If bootstrap values were < 65 and posterior probabilities < 0.85 , the symbol “+” were used. The taxon that could not be identified at genus-level on the sole basis of molecular analysis is shown in boldface and overlined in grey.

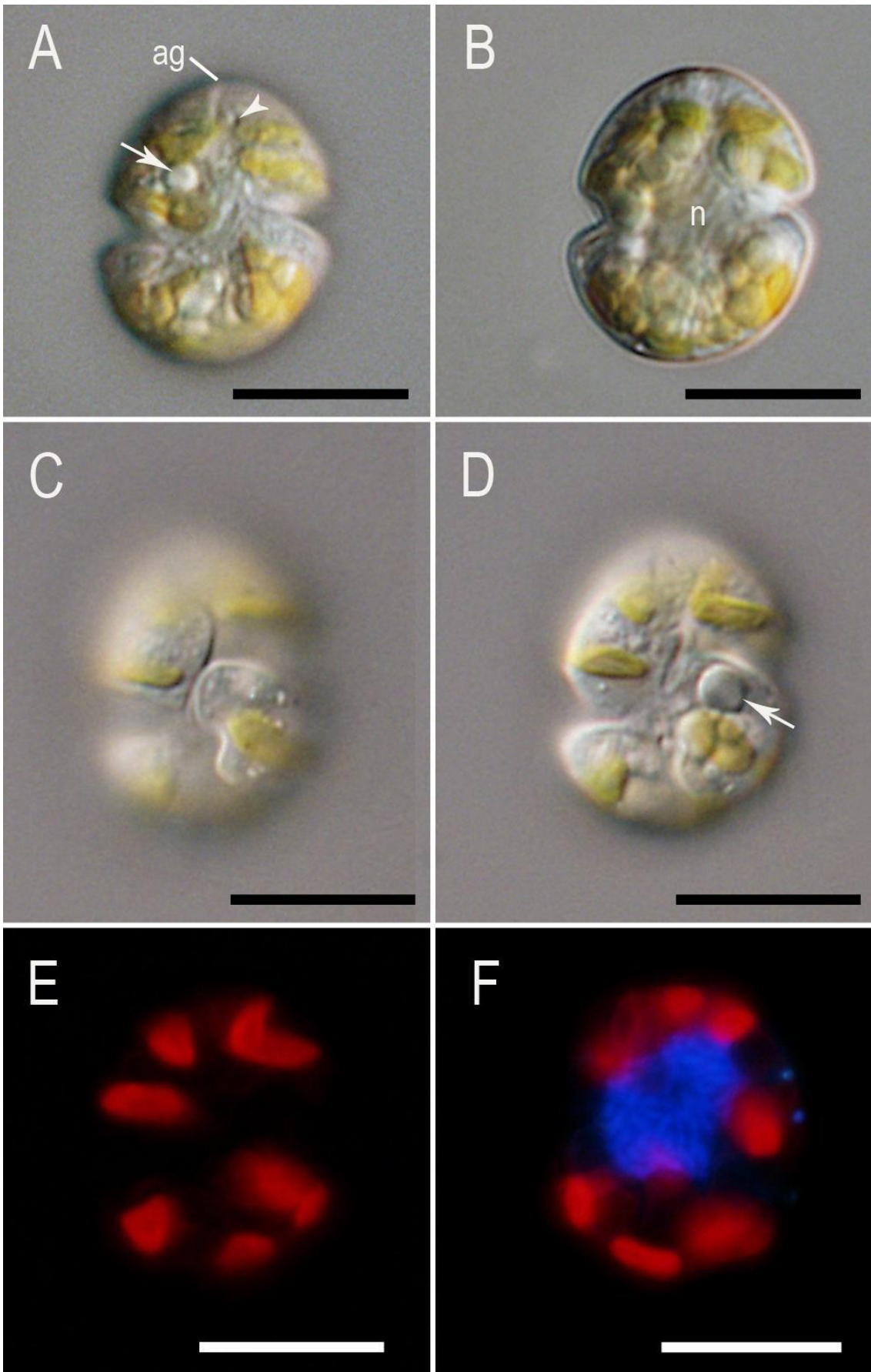


Fig. 4. Light and epifluorescence micrographs of *Karlodinium gentienii* sp. nov. (strain IFR-KGE-01C). (A) Ventral view of a cell showing the apical groove (ag), the ventral pore (arrowhead), and a refractive body (arrow). (B) Cell in median focus showing the central position of the nucleus (n). (C) Surface focus of cell in ventral view showing the furrows. (D) Ventral view showing the color and the shape of the chloroplasts, and a refractive body (arrow). (E) Cell in epifluorescence microscopy showing the peripheral and irregularly shaped chloroplasts. (F) DAPI-stained cell showing the autofluorescent chloroplasts (red) and the nucleus (blue). Scales bars = 10 μ m.

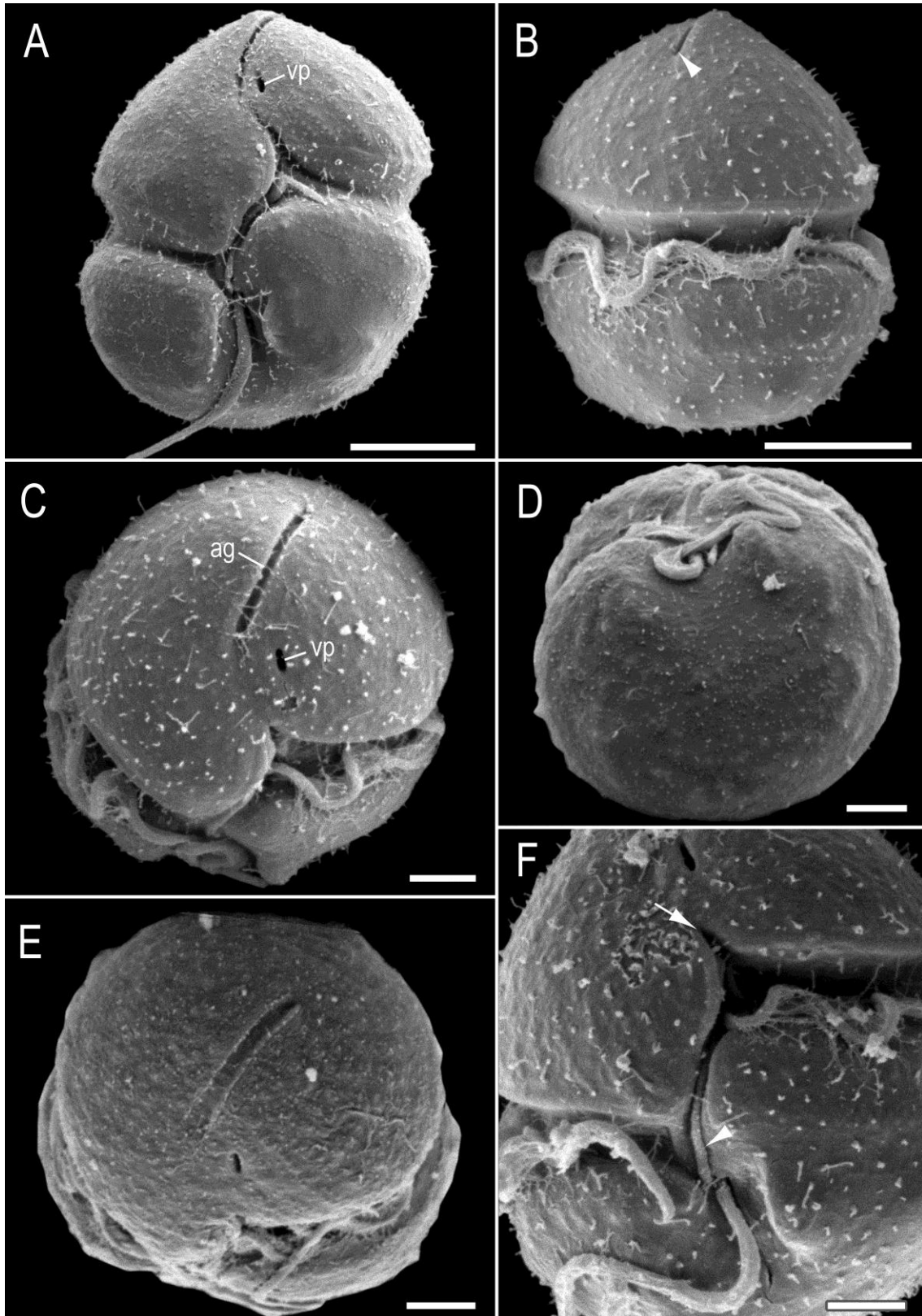


Fig. 5. SEM micrographs of *Karlodinium gentienii* sp. nov. (strain IFR-KGE-01C). Cells fixed with 2 % OsO₄ and 0.5 % glutaraldehyde (final concentrations). (A) Ventral view showing the ventral pore (vp) and the arrangement of furrows. (B) Dorsal view showing the dorsal end of the apical groove (arrowhead). (C) Cell showing the apical groove (ag) and the ventral pore (vp). (D) Antapical view showing a slight dorsoventral compression. (E) Apical view showing the apical groove directed obliquely. (F) Detail of the sulcal region. Note the finger-like protusion on the epicone (arrow) and the peduncle-like in the intercingular region (arrowhead). Scale bars: (A and B) 5 μ m, (C, D, E and F) 2 μ m.

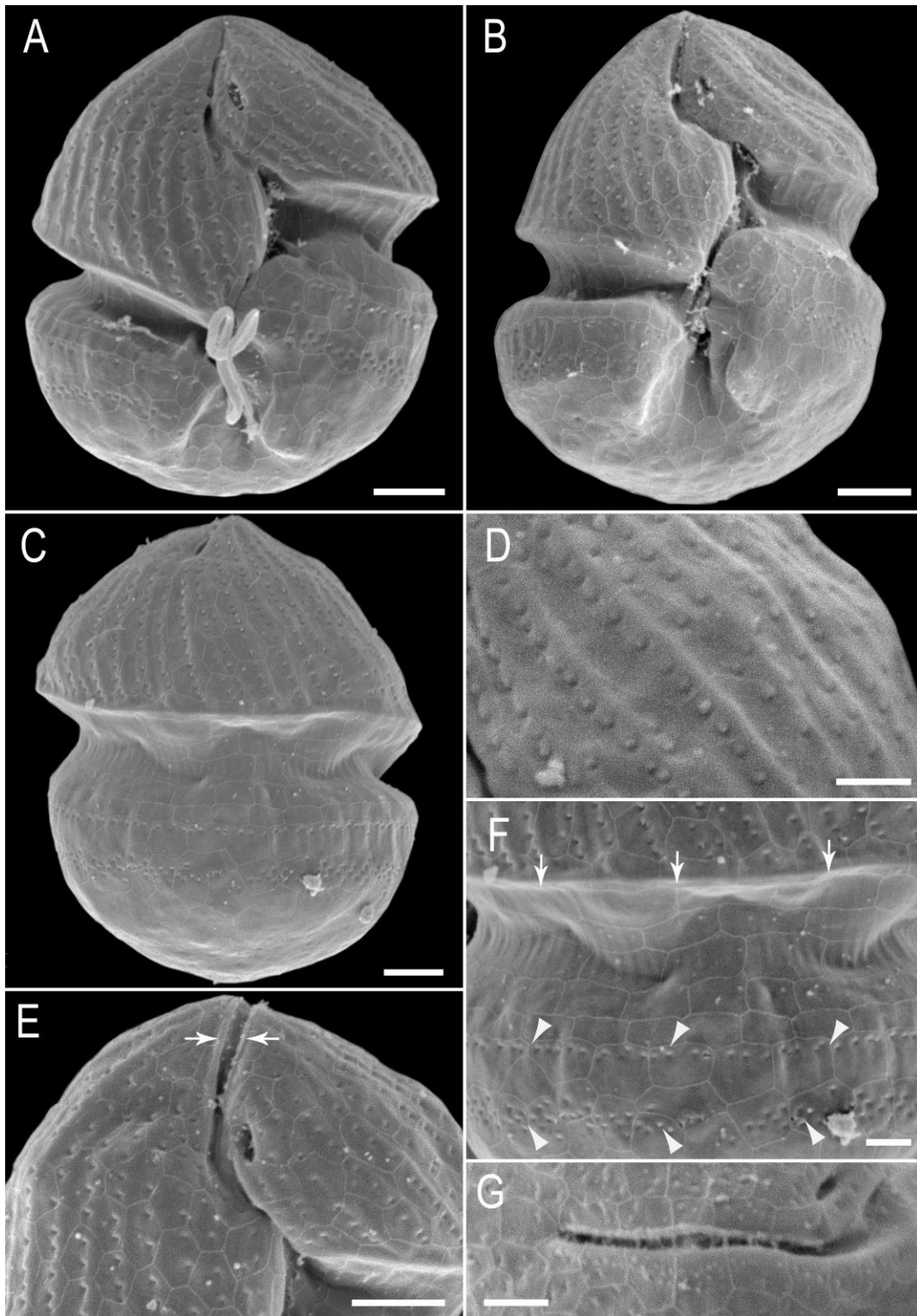


Fig. 6. SEM micrographs of *Karlodinium gentienii* sp. nov. (strain IFR-KGE-01C). Cells fixed with 1 % acidic Lugol's solution and 1 % glutaraldehyde (final concentrations). (A-B) Ventral views. (A) Parallel spiral furrows on the epicone. (B) Polygonal amphiesmal vesicles covering entirely the cell surface. (C) Dorsal view. (D) Detail of the parallel corrugations and rows of rounded structures on the epicone. (E). Detail of the apical groove with a focus on the thick margins (arrows). (F). Detail of the amphiesmal structure with a focus on the vesicles, the anterior rim of the cingulum (arrows) and the two striae of knobs at cell surface of the hypocone (arrowheads). (G). Apical groove with a focus on the amphiesmal vesicles. Scale bars: (A, B, C and E) 2 μm , (D, F and G) 1 μm .

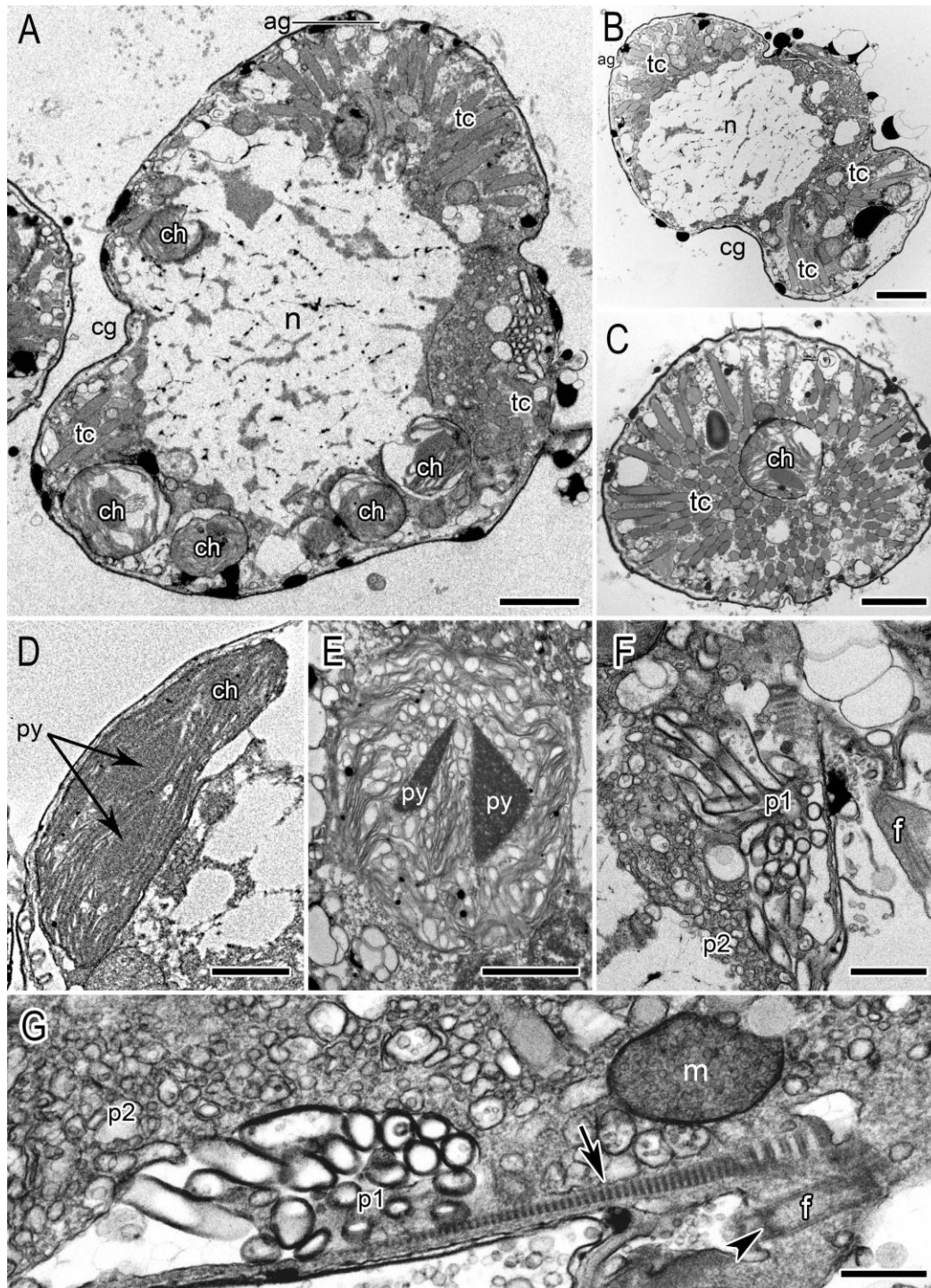


Fig. 7. TEM micrographs of *Karlodinium gentienii* sp. nov. (strain IFR-KGE-01C). (A-B) Longitudinal sections of a cell in ventral view (A) and in lateral view (B), showing the nucleus (n) and the peripheral chloroplasts (ch). The cingulum (cg) and the apical groove (ag) rims are evident. The array of trichocyst cisternae (tc) are concentrated above the nucleus and below the cingulum. (C) Cross section through a cell above the nucleus, showing the trichocyst cisternae (tc) extending from the inner part of the cell toward the cell membrane. (D-E) Chloroplasts with pyrenoids (py) appearing lenticular in longitudinal section (D) and triangular in cross section (E). (F-G) Sections through the pusule system and the flagellar apparatus. Note that the tubes forming the pusule system (p1 and p2) are of two size classes. One flagellum (f), a striated root (arrow), a flagellar base (arrowhead), and a mitochondrion (m) are visible. Scale bars: (A, B and C) 2 μ m, (D, E and F) 1 μ m, (G) 500 nm.

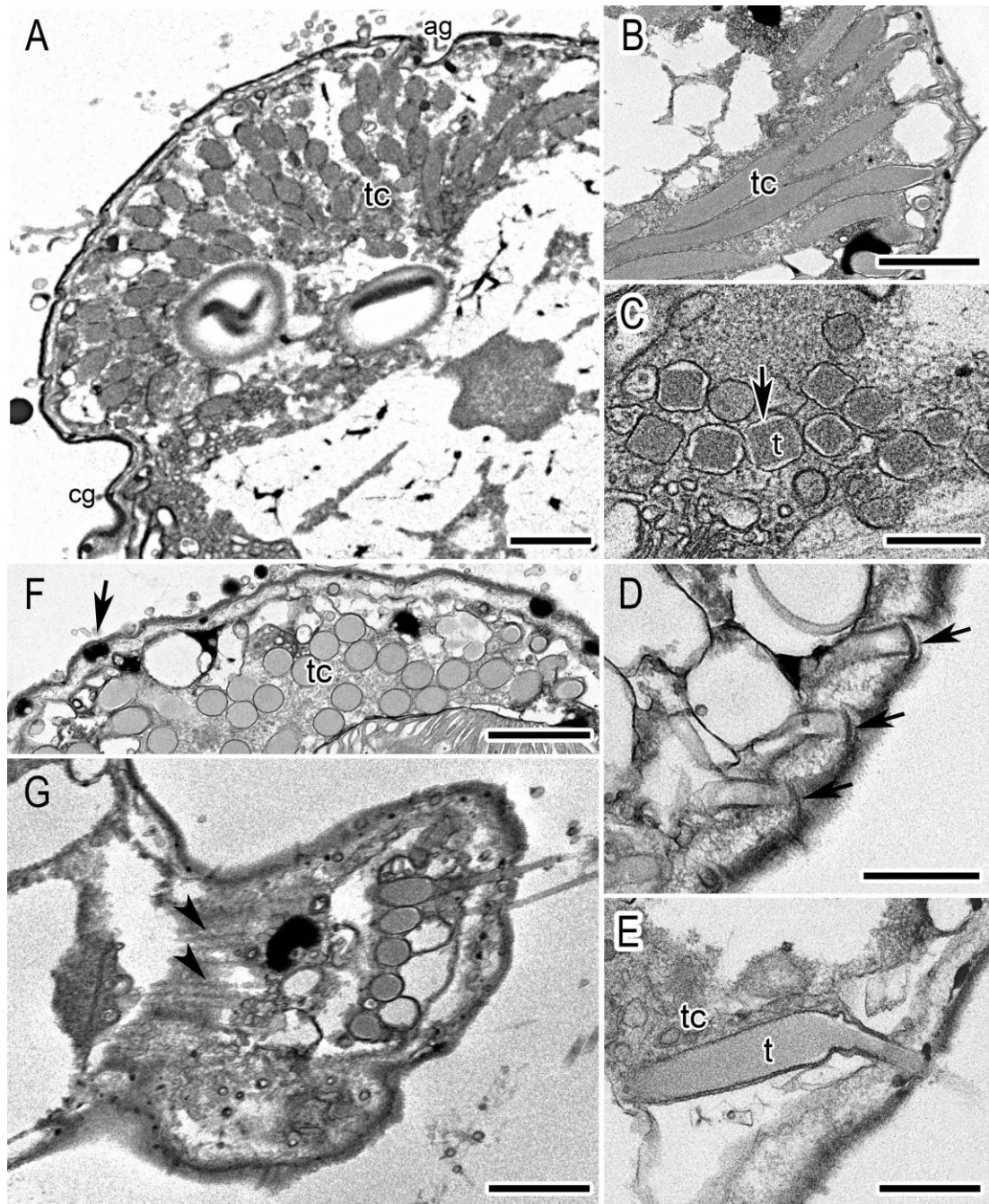


Fig. 8. TEM micrographs of *Karlodinium gentienii* sp. nov. (strain IFR-KGE). Details of the trichocyst system and the amphiesma. (A-F) Trichocyst cisternae (tc). (A) Array located in the epicone. (B) Cisternae in longitudinal section. (C) Distal part of cisternae in cross section. Note that the trichocysts (t) detach from the cisternae wall (arrow). (D) Lid-like structures covering the trichocyst exits (arrows). (E) A trichocyst during discharge. Note that the lid-like structure is raised. (F) Cross section of cisternae near the amphiesma. Note lipidic droplets within the amphiesma (arrow). (G) Tangential section through the amphiesma. Note the bundles of microtubules (arrowheads). Ag = apical groove; cg = cingulum. Scale bars: A, B, F and G = 1 μ m, C, D and E = 500 nm.

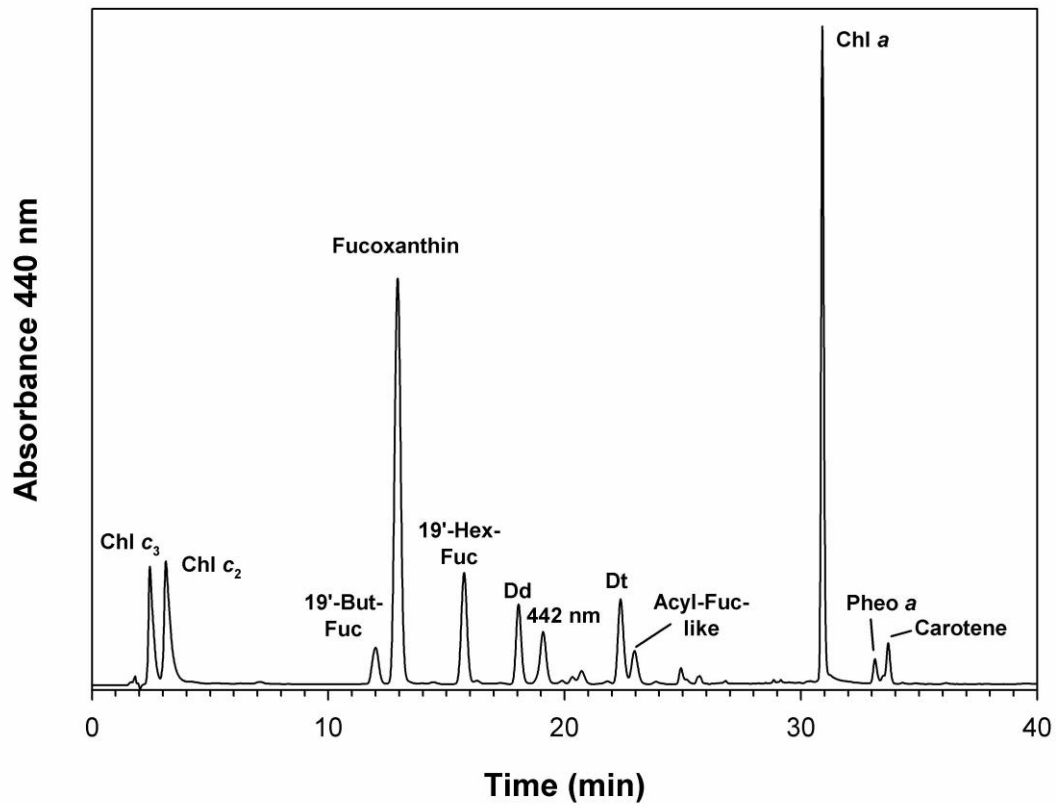


Fig. 9. HPLC chromatogram (absorption at 440 nm) of a *Karlodinium gentienii* culture in exponential growth phase, grown under low light irradiance. Note the absence of non-polar chl c and gyroxanthin derivatives. 19'-But-Fuc: 19'-Butanoyloxyfucoxanthin; 19'-Hex-Fuc: 19'-Hexanoyloxyfucoxanthin; Dd: diadinoxanthin; Dt: diatoxanthin; Acyl-Fuc-like: Acyl-fucoxanthin-like compound; Pheo a: pheophytin a.

Table 2. Estimated ranges of genetic distances (pairwise) between partial LSU rDNA (D1-D2) sequences calculated between individuals (strains) of the same species and between species in the same genus

Taxa	n	min	max	average distance between taxa
Average between 8 species of <i>Karenia</i>	46	0.029	0.090	
<i>Karenia mikimotoi</i>	22	0.000	0.003	
<i>Karenia brevis</i>	7	0.000	0.001	
<i>Karenia papilionacea</i>	6	0.001	0.016	↕ 0.029
* <i>Karenia</i> sp1	2*	0.000	0.000	
<i>Karenia umbella</i>	5	0.000	0.003	↕ 0.012
* <i>Karenia</i> sp2	3*	0.000	0.000	
<i>Karenia brevisulcata</i>	2	0.000	0.000	
<i>Karenia cristata</i>	2	0.000	0.000	
<i>Karenia selliformis</i>	1	—	—	
<i>Karenia bidigitata</i>	1	—	—	
Average between 9 species of <i>Karlodinium</i> (excluding <i>K. antarcticum</i> and <i>K. decipiens</i>)	27	0.020	0.099	
<i>Karlodinium veneficum</i>	14	0.000	0.015	
<i>Karlodinium armiger</i>	3	0.000	0.011	
<i>Karlodinium ballatinum</i>	3	0.000	0.007	↕ 0.028
<i>Karlodinium gentienii</i> sp. nov.	2	0.000	0.000	
<i>Karlodinium</i> sp. (strain KAMS0708)	1	—	—	↕ 0.027
<i>Karlodinium australe</i>	2	0.000	0.003	
<i>Karlodinium conicum</i>	1	—	—	
<i>Karlodinium corrugatum</i>	1	—	—	↕ 0.027
* <i>Karlodinium</i> sp. (isolates IFR797/981)	2*	0.000	0.000	

Average between 5 species of <i>Takayama</i>	11	0.011	0.040	
<i>Takayama acrotrocha</i> **	4	0.018	0.032	
<i>Takayama xiamenensis</i>	3	0.000	0.000	
<i>Takayama helix</i>	1	—	—	
<i>Takayama tuberculata</i>	1	—	—	
<i>Takayama tasmanica</i>	3	0.000	0.000	
* <i>Takayama</i> sp.	2*	0.000	0.000	↕ 0.004

*Sequences of unidentified species acquired in this study were not included in the calculation of average p-distances between species within the same genus.

**Sequences of *T. acrotrocha* available in Genbank show a very high level of divergence even in conserved parts of the alignment.

Table 3: Morphological characters of *Karlodinium gentienii*, in comparison with other *Karlodinium* species.

	<i>Karlodinium gentienii</i>	<i>Karlodinium corsicum</i> ^a	<i>Karlodinium veneficum</i> ^b (K-0522)	<i>Karlodinium armiger</i> ^b	<i>Karlodinium australe</i> ^c	<i>Karlodinium antarcticum</i> ^d	<i>Karlodinium ballantinum</i> ^d _e	<i>Karlodinium conicum</i> ^d	<i>Karlodinium corrugatum</i> ^d	<i>Karlodinium m. decipiens</i> ^d
Cell length (µm)	13.5–18.9 (16.3 ± 1.5, n=30)	17–24	8–18 (13.6 ± 1.9, n=50)	12–22 (17.4 ± 2.4, n=50)	19–26 (21.8 ± 1.8, n=30)	15–24 (19.2 ± 0.2, n=76)	11–18 (14.6 ± 0.2, n=73)	19–29 (24.3 ± 0.2, n=80)	13–21 (16.2 ± 0.1, n=100)	18–25 (21.4 ± 0.2, n=50)
Cell width (µm)	11.5–16.8 (13.6 ± 1.4, n=30)	12–16	8–14 (11.1 ± 1.4, n=50)	8–18 (13.1 ± 1.8, n=50)	16–22 (18.9 ± 1.8, n=30)	10–14 (12.0 ± 0.1, n=76)	8–14 (10.9 ± 0.2, n=73)	15–25 (19.9 ± 0.2, n=80)	11–17 (13.9 ± 0.1, n=100)	13–19 (16.2 ± 0.2, n=50)
Length to width ratio	1.11–1.33 (1.20 ± 0.05, n=30)	1.21 ^f	0.97–1.49 (1.23 ± 0.1, n=50)	1.15–1.55 (1.33 ± 0.1, n=50)	1.14 ^f	1.36–2.12 (1.60 ± 0.01, n=76)	1.20–1.58 (1.35 ± 0.01, n=73)	1.05–1.39 (1.22 ± 0.01, n=80)	0.99–1.36 (1.17 ± 0.01, n=100)	1.15–1.55 (1.32 ± 0.01, n=50)
Girdle displacement (% cell length)	25–31	32–34	23–32	29–36	25	20–33	33	25	25	33
Sulcal extension	Yes	Yes	Yes	Yes	Yes	Inconspicuous or absent	Short but evident	Yes	Yes	Inconspicuous fold
Apical groove	Linear, descending one-sixth down the dorsal epicone	With a curved base, descending one-third down the dorsal epicone	Straight, descending one-seventh down the dorsal epicone	Straight, descending one-fourth down the dorsal epicone	Short and straight, extending only briefly onto the dorsal epicone	Very long, extending halfway down the dorsal epicone	Very short and linear, extending very briefly onto the dorsal epicone	Relatively short, extending one-fourth down the dorsal epicone	Medium sized, extending approximately one-third down the dorsal epicone	Long, extending halfway down the dorsal epicone
Ventral pore	Elongated (0.8–1.0 µm), above the sulcal intrusion, next to the base of the carina	Kidney-shaped, next to the curved base of the apical groove	Elongated (1µm) to the left of the apical groove	Elongated (1µm) to the left of the apical groove	Reniform, above and to the left of the sulcal intrusion	Inconspicuous or absent	Absent or inconspicuous	Conspicuous and round, halfway between the sulcal termination and the	Slit-like, located far to the left of the sulcal region and the carina	Slit-like, located above the sulcus

Amphiesma structure	Polygonal vesicles, numerous rows of micro-structures on the epicone and only 2 rows below the cingulum, numerous trichocysts dischargeable in the epicone and below the cingulum, no evidence of plugs	Granulated, smoother on the hypocone, numerous micro-structures irregularly arranged on the epicone and two parallel rows on the hypocone	Numerous minor depressions arranged in rows, every depression comprising a plug	Vesicles with a granulated structure, numerous rounded structures randomly placed, numerous trichocysts dischargeable in the epicone, no evidence of plugs	Hexagonal vesicles, no pores on the surface, parallel microtubular bands, no evidence of plugs	n.a.	Two striae of knobs, one on the epicone and the other one on the hypocone	beginning of the carina n.a.	n.a.	n.a.
---------------------	---	---	---	--	--	------	---	---------------------------------	------	------

Table S1. List of sequences used for p-distances calculations (on D1-D2 region) in table 2.

species	strain/isolate	origin	Genbank accession number
<i>Karenia mikimotoi</i>	AC213	—	HM807332
	CCMP430	—	HM807333
	CCMP429/PLY497a	—	AF200678
	K-0286	Australia	AF200679
	KMWL01	Australia	EF469238
	K-0579	Denmark	AF200682
	GATIN95	France, Atlantic	KJ508362
	IFR559	France, Atlantic	KJ508363
	IFR980	France, Mediterranean	KJ508361
	?	Japan	AF200681
	MBA561	Japan	HM807325
	GMKUSJAP CAWD05	Japan	U92247
	IFR11-056	New Caledonia	KJ508365
	CAWD117	New Zealand	HM807326
	CAWD133	New Zealand	HM807327
	CAWD134	New Zealand	HM807328
	G01WAINZ, IS02	New Zealand	U92249
	KT77B		AF200680
	K-0260	Norway	HM807331
	IFR13-379	Saint-Pierre-and-Miquelon	KJ508364
CCMP429	United Kingdom	HM807329	
NOAA-2	USA, Florida	AY355460	
<i>Karenia brevis</i>	Jacksonville C3-5	—	DQ847431
	GRHIUS CAWD08	New Zealand	U92248
	JL32	USA, Florida	AF200677
	PNS	USA, Florida	AY355457
	JaxC5	USA, Florida	AY355459
	Texas B5	USA, Texas	AY355455
	sp3	USA, Texas	AY355456
<i>Karenia papilionacea</i>	KPMB11	Australia, Tasmania	AY590124
	IFR562	France, Atlantic	KJ508366
	KAGAWA-15	Japan	AB771743
	G01HAWNZ, IS16	New Zealand	U92252
	VGO679	Spain	FN649411
	IFR13-294	St-Pierre-and-Miquelon	KJ508367
<i>Karenia</i> sp1	IFR572	France, Atlantic	KJ508374
	IFR528	France, Atlantic	KJ508373
<i>Karenia umbella</i>	KUSR01	Australia	EF469239
	KUTN05	Australia, Tasmania	AY263963
	KULV01	Australia, Tasmania	AY263962
	IFR644	France, Atlantic	KJ508368
	IFR13-377	Saint-Pierre-and-Miquelon	KJ508372
<i>Karenia</i> sp2	IFR868	France, Mediterranean	KJ508369
	IFR1186	France, Mediterranean	KJ508370

<i>Karenia brevisulcata</i>	IFR-KUM-01U	France, Corsica	KJ508371
	IFR1133	France, Atlantic	KJ508359
		New Zealand	AY243032
<i>Karenia cristata</i>	IFR13-067	Saint-Pierre-and-Miquelon	KJ508360
		South Africa	AY243963
<i>Karenia selliformis</i>	CAWD37	New Zealand	U92250
<i>Karenia bidigitata</i>	CAWD81	New Zealand	AY947663
<i>Karlodinium veneficum</i>	KDMPT01	Australia	AY263964
	IFR10-150	France, Atlantic	KJ508380
	IFR10-101	France, Atlantic	KJ508382
		France, Corsica	AF318249
	IFR-KVE-01D	France, Corsica	KJ508381
	MC710-A1	Italy	FJ024701
	IFR11-130	New Caledonia	KJ508384
	CAWD84	New Zealand	AY947665
	G01WHKNZ IS03	New Zealand	U92257
	K-0522	Norway	AF200675
	RCC2539	Norway	KJ508383
	BgT1	Tunisia	DQ898222
	Plymouth-103	United Kingdom	DQ114466
	Pim05JulC4	USA, Florida	AY245692
<i>Karlodinium armiger</i>	K-0668	—	DQ114467
	IFR10-093	France, Atlantic	KJ508376
	IFR-KAR-01D	France, Corsica	KJ508375
<i>Karlodinium ballantinum</i>	KDBMP01	Australia, Tasmania	EF469232
	MC701-B1	Italy	FJ024699
	MC728-A1	Italy	FJ024700
<i>Karlodinium gentienii</i>	IFR-KGE-01C	France, Atlantic	KJ508379
	IFR10-074	France, Atlantic	KJ508378
<i>Karlodinium</i> sp.	KAMS0708	Korea	FN357291
<i>Karlodinium australe</i>	KDATL11	Australia	DQ151560
	GT5	Singapore	DQ156228
<i>Karlodinium conicum</i>	KDCSO15	Australia	EF469231
<i>Karlodinium corrugatum</i>	KDGSO08	Australia	EF469233
<i>Karlodinium</i> sp.	IFR797	France, Atlantic	KJ508385
	IFR981	France, Mediterranean	KJ508386
<i>Takayama acrotrocha</i>	CCMP2960	Singapore	HQ834208
	clone GT17	Singapore	DQ656117
	clone GT15	Singapore	DQ656116

	clone GT7	Singapore	DQ656115
<i>Takayama xiamenensis</i>	GSXM03	China	KC485078
	MC728-D5	Italy	FJ024703
	MC728-B4	Italy	FJ024702
<i>Takayama helix</i>	TTNWB01	Australia	AY284950
<i>Takayama tuberculata</i>	TTBSO11.1	Australia	EF469230
<i>Takayama tasmanica</i>	TTTL02	Australia	AY284949
	TTDE01	Australia, Tasmania	AY284948
	TTLJ01	China	KC485077
<i>Takayama</i> sp.	IFR863	France, Atlantic	KJ508387
	IFR909	France, Atlantic	KJ508388

Table S2. Presence/absence of gyroxanthin and non polar-chl c_2 derivatives among 35 *Karlodinium* strains of 5 species. The symbol + indicates the presence of the pigment, the symbol – indicates the absence. Gyro: gyroxanthin.

Species	Strain	Gyro derivatives	Non polar-chl c_2	Reference
<i>K. armiger</i>	GC-2	+	+	Garcés et al. (2006)
<i>K. armiger</i>	GC-3	+	+	Garcés et al. (2006)
<i>K. armiger</i>	GC-7	+	+	Garcés et al. (2006); Zapata et al. (2012)
<i>K. armiger</i>	K-0668	+	?	Bergholtz et al. (2006)
<i>K. australe</i>	KDAGT03	–	+	De Salas et al. (2005)
<i>K. australe</i>	KDATL05	–	+	De Salas et al. (2005)
<i>K. australe</i>	KDAPP01	–	+	De Salas et al. (2005)
<i>K. decipiens</i>	Nervion34	+	+	Zapata et al. (2012)
<i>K. gentienii</i>	IFR-KGE-01C	–	–	This study
<i>K. veneficum</i>	RCC2539	+	–	This study
<i>K. veneficum</i>	CCMP1974	+	–	Kempton et al. (2002); Zapata et al. (2012)
<i>K. veneficum</i>	CCMP1975	+	–	Bachvaroff et al. (2009)
<i>K. veneficum</i>	CCMP2388	+	–	Bachvaroff et al. (2009)
<i>K. veneficum</i>	CCMP2282	+	–	Bachvaroff et al. (2009)
<i>K. veneficum</i>	CCMP2283	+	–	Bachvaroff et al. (2009)
<i>K. veneficum</i>	CCMP2064	+	–	Bachvaroff et al. (2009)
<i>K. veneficum</i>	010410-C6	+	–	Kempton et al. (2002)
<i>K. veneficum</i>	CCMP415	+	–	Zapata et al. (2012)
<i>K. veneficum</i>	CCMP2778	+	–	Bachvaroff et al. (2009)
<i>K. veneficum</i>	CS-310	+	–	Zapata et al. (2012)

<i>K. veneficum</i>	GC-1	+	-	Garcés et al. (2006)
<i>K. veneficum</i>	GC-4	+	-	Garcés et al. (2006); Zapata et al. (2012)
<i>K. veneficum</i>	GC-5	+	-	Garcés et al. (2006)
<i>K. veneficum</i>	VGO691	+	-	Zapata et al. (2012)
<i>K. veneficum</i>	VGO870	+	-	Zapata et al. (2012)
<i>K. veneficum</i>	MD2	+	-	Bachvaroff et al. (2009)
<i>K. veneficum</i>	MD5	+	-	Bachvaroff et al. (2009)
<i>K. veneficum</i>	MD6	+	-	Bachvaroff et al. (2009)
<i>K. veneficum</i>	Slocum	+	-	Bachvaroff et al. (2009)
<i>K. veneficum</i>	MBM1	+	-	Bachvaroff et al. (2009)
<i>K. veneficum</i>	IB4	+	-	Bachvaroff et al. (2009)
<i>K. veneficum</i>	PD-6	+	-	Bachvaroff et al. (2009)
<i>K. veneficum</i>	F4	+	-	Bachvaroff et al. (2009)
<i>K. veneficum</i>	CAWD66	+	-	Bachvaroff et al. (2009)
<i>K. veneficum</i>	CAWD83	+	-	Bachvaroff et al. (2009)
